

Optimal planning and feedstock-mix selection for multiproduct polymer production

Pablo A. Marchetti^a, Miguel A. Zamarripa^b, Juan A. Reyes-Labarta^c,
Ignacio E. Grossmann^{b,*}, Wiley Bucey^d, Rita A. Majewski^d

^a Instituto de Desarrollo Tecnológico para la Industria Química (UNL-CONICET), Güemes 3450, 3000 Santa Fe, Argentina

^b Carnegie Mellon University, Chemical Engineering Dept., Pittsburgh, PA 15213, USA

^c Departamento de Ingeniería Química, Universidad de Alicante, Apartado de Correos 99, 03080 Alicante, Spain

^d Braskem America, Pittsburgh, PA 15219, USA

ARTICLE INFO

Article history:

Received 23 March 2016

Received in revised form 1 September 2016

Accepted 1 September 2016

Available online 8 September 2016

Keywords:

Polymer production

Polymer scheduling

Continuous processes

Plant and process optimization

ABSTRACT

In this paper, we describe a nonlinear programming model to determine the optimal balance of feedstocks to manufacture multiple polymer grades in a polypropylene production facility. The main units of the process are a distillation column and a polymerization reactor, for which accurate short-cut process models were developed. Both a single and multiple product formulations are presented. The proposed models seek to maximize the plant throughput while minimizing the production costs. The possibility of adding extra production is also considered. The formulations are applied to several case studies, both to analyze the performance of the model and to illustrate its potential economic impact. The trade-off between feedstocks costs and production rates is analyzed by solving the multiple-product model with different time horizons. An annualized-slate long term case study is presented. The proposed formulation with a user-friendly interface has been deployed to assist with commercial and operation decisions at the plant.

© 2016 Elsevier Ltd. All rights reserved.

1. Introduction

Polymer manufacturing is a continuous process where several campaigns of different product families are scheduled in a cyclic manner. The raw materials, usually referred as ‘feedstock’, are by-products of petroleum or natural gas such as ethylene and propylene, and their prices are inextricably linked to the prices of such commodities. The polymer market is extremely competitive and the quality expectation of customers is very high. Polymer plants usually operate at full capacity, seeking to improve the return on assets and reduce the supply chain costs (Kadipasaoglu et al., 2008).

Polypropylene plants typically produce several different product grades and are able to achieve different maximum production rates due to a variety of constraints. Efficiency is extremely important because the cost of downtime and transition time with off-spec production is extremely high (of the order of dollars per second). Thus, shutdowns and large transitions should be eliminated or reduced whenever possible. To handle this situation, production

schedules are prepared with the order of products following an idealized production wheel based on the most efficient transition policy, while the length of the cycle leads to efficient customer service and avoids excessive inventory by adjusting production frequency. A schedule is typically projected a few months into the future, and includes 10 to 30 campaigns in a cycle, each campaign including the production of a family of products (5–30 different products per family). Fig. 1 shows a simplified production wheel with five families of products in a particular sequence (‘A’ to ‘B’ to ‘C’ to ‘D’ to ‘E’ and start again with ‘A’).

Polypropylene plants may be supplied with three different grades of monomer:

- Polymer grade or PGP (99.5 wt% propylene)
- Chemical grade or CGP (92–96 wt% propylene)
- Refinery grade or RGP (50–80 wt% propylene)

The cost of propylene is substantially lower for RGP compared to chemical and polymer grade. For instance, historical RGP to CGP spreads can vary anywhere from 8 to 25 cents per pound (cpp). If a polypropylene plant receives different grades of monomer (e.g. RGP and CGP), the best operating conditions can be chosen taking into account the difference on monomer prices. While in terms of

* Corresponding author.

E-mail address: grossmann@cmu.edu (I.E. Grossmann).

Nomenclature*Subscripts*

c	Cascade of trays
i	Component
j	Distillation unit tray
k	Production time slot
k^+	Production time slot for slack product
n	Polymerization reactor loop/vessel
p	Product grade
q	Mixer or splitter
s	Stream

Sets

I	Components
I_s^{eq}	Components of stream s with fixed composition
I_s^{lb}, I_s^{ub}	Components of stream s with constrained composition (lower or upper bounds)
K	Production time slots
MX	Mixers
P	Products
S	Streams
$S_{q,in}, S_{q,out}$	Input and output streams, respectively, of mixer or splitter q
SP	Splitters

Parameters

C_0	Initial number of active sites per unit catalyst
c_s	Feedstock costs ($s = RG$ or $s = CG$)
$c_p^{catalyst}$	Cost of catalyst for product p
K_p	Kinetic rate constant for product p
K_p^0	Propagation rate constant for product p
KD_p	Deactivation rate constant for product p
$price_p$	Market price of polypropylene product p
r_s	Market return price ($s = DB$)
SL^{max}	Maximum extra production allowed
V	Loop volume
β_n	Discharge factor for loop n
θ_1, θ_2	Linear coefficients to approximate distillation overhead composition
ρ_S	Solids density (density of polypropylene)
ρ_{SL}	Slurry density
$\sigma_{s,i}$	Fixed composition for component i at stream s
$\sigma_{s,i}^{min}, \sigma_{s,i}^{max}$	Minimum and maximum compositions for component i at stream s
$\phi_s^{min}, \phi_s^{max}$	Minimum and maximum flowrate of stream s
φ	Centrifugation fraction

Variables

$A_{e,i}$	Effective absorption factor of component i for an average tray of the cascade ($A_{e,i}^c$ for cascade c)
$A_{j,i}$	Absorption factor of component i at tray $j \in \{1, N\}$ ($A_{j,i}^c$ for cascade c)
F_s	Overall flowrate of stream s
$f_{s,i}$	Flowrate of component i on stream s
$H_{j,i}^L$	Enthalpy of liquid flow of component i leaving tray j
$H_{j,i}^V$	Enthalpy of gas flow of component i leaving tray j
$K_{j,i}$	K-value for component i at tray j ($K_{j,i}^c$ for cascade c)
L_j	Liquid flow leaving tray j (L_j^c for cascade c)
$L_{j,i}$	Liquid flow of component i leaving tray $j \in \{0, N\}$ ($L_{j,i}^c$ for cascade c)
MK	Makespan

R	Production rate of polypropylene
R_n	Polypropylene production rate in loop n
$S_{e,i}$	Effective stripping factor of component i for an average tray of the cascade ($S_{e,i}^c$ for cascade c)
$S_{j,i}$	Stripping factor of component i at tray $j \in \{1, N\}$ ($S_{j,i}^c$ for cascade c)
t_j	Temperature at tray j
T_k	Processing time of time slot k
V_j	Gas flow leaving tray j (V_j^c for cascade c)
$V_{j,i}$	Gas flow of component i leaving tray $j \in \{1, N+1\}$ ($V_{j,i}^c$ for cascade c)
w_n	Solids fraction in the outlet of loop n
x_{DO}	Propylene composition in distillation overhead
x_n	Weight fraction of propylene in the reactor slurry at loop n
x_{RF}	Propylene composition in reactor feed
Y_n	Catalyst yield in loop n
κ	Catalyst flow (κ^k for time slot k)
$\rho_{L,n}$	Density of liquid in loop n
τ_n	Residence time in loop n
$\phi_{A,i}, \phi_{S,i}$	Recovery factors for absorption and stripping, respectively, for component i ($\phi_{A,i}^c$ and $\phi_{S,i}^c$ for cascade c)

Aggregated variables

Q	Flowrates matrix (Q^k for time slot k)
Q_s	Flowrates vector for stream s
U	Collection of vectors μ_c for every cascade c (U^k for time slot k)
v_n	Vector of variables for loop n
V	Collection of variables modelling the polymerization reactor (V^k for time slot k)
η_i	Vector of component i variables for a cascade of trays (η_i^c for cascade c)
μ_c	Collection of variables for cascade c
$\mu_{c,j}$	Vector of vapor and liquid flowrates between tray j and tray $j+1$ at cascade c

cost RGP is the preferred feedstock, there is a tradeoff between feedstock purity and polymer production rate due to the numerous process constraints. Nonetheless, selecting the optimal balance of feedstocks and plant operating conditions for a given monomer spread can lead to substantial savings on the production cost.

Over the last decades, significant progress has been made in the development of new optimization models and computational tools to solve real industrial applications. In the context of Enterprise-wide Optimization, Grossmann (2005, 2012) reviewed the contributions in planning and scheduling of production facilities and supply chains applications. Also, an overview of the modelling approaches (i.e. discrete vs. continuous time representations, sequence dependence vs. precedence based models, etc.), decisions involved (allocation, sequencing and timing decisions), and solution methods (MILP and MINLP), with examples of industrial applications can be found in the last scheduling review by Harjunkoski et al. (2014). Most of the chemical engineering contributions involving planning or scheduling problems do not use process models, replacing them with parameters like fixed processing rates and fixed processing times (Kondili et al., 1993; Floudas and Lin, 2004; Méndez et al., 2006a; Castro et al., 2009; Sundaramoorthy and Maravelias, 2011).

While linear models are still common for planning and scheduling applications, it is clear that these problems often require a

more detailed process description (Grossmann, 2012). For instance, a common nonlinear example is the blending problem, in which the process representation involves bilinear terms in the mass balance equations (Méndez et al., 2006b; Mouret et al., 2009; Kolodziej et al., 2013). Another example is cyclic scheduling in which the objective function must be divided by the cycle time (Pinto and Grossmann, 1994; Wu and Ierapetritou, 2004; You et al., 2009). Given the advances in NLP solvers (e.g. SNOPT, CONOPT, IPOPT, and BARON) and MINLP solvers (DICOPT, SBB, α -ECP, and BARON), there is an increasing number of computational tools to solve nonlinear optimization problems (Nocedal and Wright, 2006; Belotti et al., 2013).

Nonlinear process models are also used at lower decision levels such as real time optimization (RTO), which usually requires first-principles nonlinear formulations to represent steady state operating conditions, and model predictive control (MPC), which introduces differential algebraic equations (DAE) to represent the process dynamics. Moreover, several methodologies integrate decisions of different hierarchical levels (such as design, planning, scheduling, RTO, or process control), which requires more complex dynamic non-linear programming formulations. Approaches such as dynamic optimization (Biegler, 2007; Biegler and Zavala, 2009) have been applied in the economic analysis for specific chemical processes such as batch distillation columns, crystallization, polymerization reactors, air separations units, etc., in order to avoid economic losses due to process disturbances, reduce the transition time between desired operating conditions, etc. However, dynamic optimization models usually require a detailed representation of kinetic mechanisms, physical transport phenomena (mass and heat), and the relationship between the operating conditions and the quality of the final product obtained, which are often not completely understood.

There is a substantial amount of research on polymerization processes and their associated mathematical modelling approaches (Kiparissides, 1996, 2006; McKenna and Soares, 2001; Soares, 2001; Almeida et al., 2008; Lin et al., 2010). Non-linear formulations, as the one needed to represent polymer production, can now be solved with reasonable computational effort. Both dynamic simulation (Touloupides et al., 2010) and optimization models (Zavala and Biegler, 2009) are concerned with the determination of control trajectories to bring a polymer reactor from an initial state to a desired final one, and are mainly applied to reactor start-up and grade transition operations. As for other highly nonlinear processes, the integration of decisions at multiple levels has also been investigated. For example, Flores-Tlacuahuac and Biegler (2008) proposed a simultaneous approach for tackling design and control problems in polymerization reactors during dynamic optimal grade transition operations. Other examples are scheduling of polymer grade transitions (Mahadevan et al., 2002) and simultaneous scheduling and control of polymerization reactors (Terrazas-Moreno et al., 2007). Unfortunately, in order to handle enterprise-wide problems the mathematical models that represent the polymerization process usually need to be simplified. As an example, simplified non-linear empirical process models were used by Jackson et al. (2003) to develop a multi-period NLP model for the production planning of a real world multi-plant polymer facility.

In this work, a non-linear programming model for the selection of the optimal balance of feedstocks for manufacturing multiple grades of polypropylene is presented. The goal is to develop a production planning tool in which the process models are explicitly incorporated to simultaneously select the operating conditions and the production rates to maximize the overall profit. The feedstocks are chemical and refinery grade propylene (propane-propylene mixture), and the process includes a distillation column and a polymerization reactor with various types of recycles. The system constraints include lower and upper bounds on flow rates, lim-

its on compositions, and limits on the catalyst yield and flow. The main decision variables are the flowrates and compositions of each stream and the catalyst flow, which based on the kinetic parameters used determine the production rates of polypropylene for each product type. The optimal operation balances the production rate with the costs of feedstocks, maximizing the plant throughput. Different products differ on how much catalyst is needed to produce a given production rate, and the objective function is driven by the economic trade-off of selling prices versus feedstock costs.

Since the separation of propane-propylene by distillation requires a large number of trays, a rigorous representation of the process gives rise to a large non-linear model. Several contributions using rigorous tray-by-tray models have been presented (e.g. Viswanathan and Grossmann, 1993; Yeomans and Grossmann, 2000; Barttfeld et al., 2003). In order to reduce the number of constraints and nonlinear terms, we avoid the use of a tray-by-tray model of a distillation column by using instead a short-cut model based on an aggregated group method (Kamath et al., 2010). This method, which models a counter-current cascade of trays without providing tray-by-tray details, was chosen in order to maintain an adequate balance between solution accuracy and model size.

A simplified nonlinear Ziegler-Natta-catalyzed polymerization model is used to describe the reactor. The model is able to represent steady-state operating conditions for each product grade. The simplified formulation assumes that the polymerization rate is proportional to the monomer concentration and the number of active catalyst sites, which in turn decays at a rate proportional to the current number of sites. Although it is well recognized that Ziegler-Natta catalysts are multi-site in character (Kissin, 2003; Zacca et al., 1996; Albizzati et al., 2005), for simplicity a single site model is used. Different product targets are distinguished by different lumped kinetic parameters, describing propagation and deactivation terms, and recipe ratios between the various components including hydrogen, propylene, cocatalyst, and electron donor. Since only steady-state operation is required, a detailed dynamic optimization approach is out of the scope of this paper.

Both a single and a multiple-product NLP optimization model are presented. The single product formulation is used as a building block to develop the multiple-product model. In the latter, a fixed time horizon is considered to produce a given schedule of polymer products. In order to obtain the optimal schedule for the multiple-product problem, we describe a solution strategy based on an aggregation/disaggregation procedure that reduces the problem dimensionality (by considering combined demands for each product family) and an initialization scheme that combines the solutions of the single product model. The models are applied to optimize the production planning simultaneously with the feedstock selection and operating conditions of the process.

The paper is organized as follows: Section 2 describes the process under consideration, and describes the problem statement and main assumptions. Section 3 presents the mathematical formulations. First, the single-product mathematical model is presented that includes an aggregated group-based method for distillation and a simplified reactor model. The multiple-product model is presented next, which is extended to allow an extra-production scenario. In Section 4 we describe the solution strategy for solving the alternative models. Finally, Section 5 presents the results obtained for several test cases and the conclusions are given in Section 6.

2. Problem statement and case study

A simplified flowsheet of the continuous process under consideration is shown in Fig. 2. The equipment includes a distillation column and a double-loop polymerization reactor, with some recy-

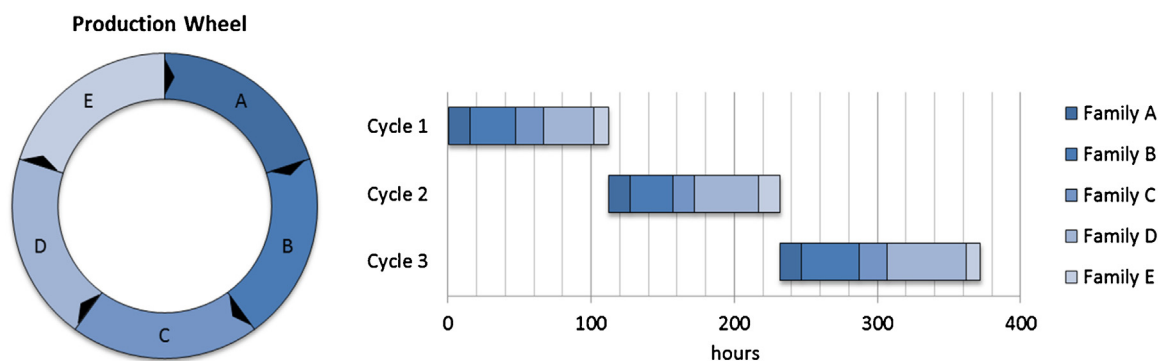


Fig. 1. Polymer manufacturing production wheel example.

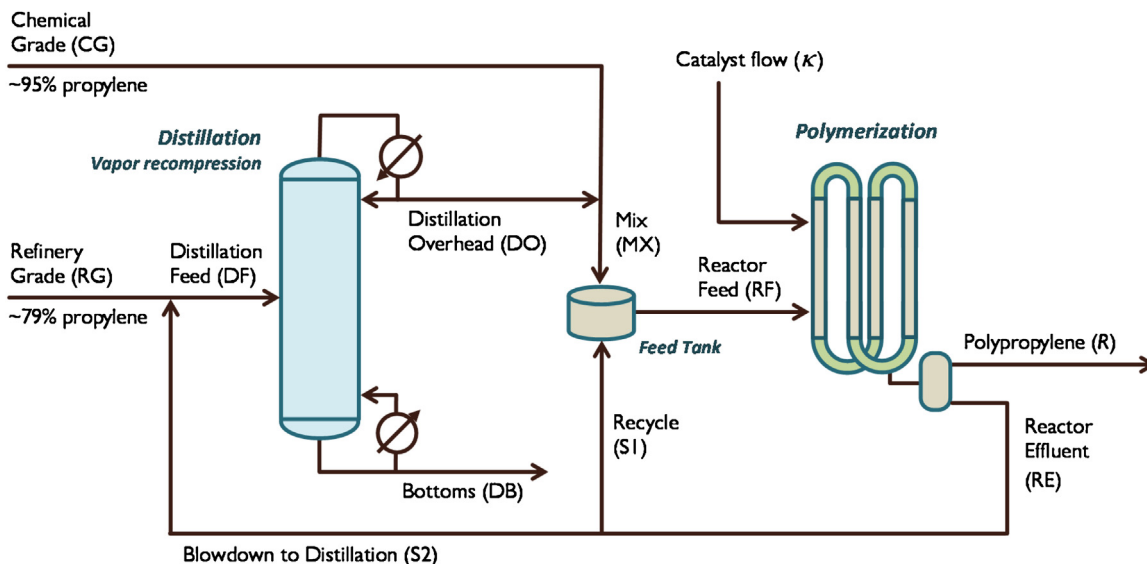


Fig. 2. Simplified flowsheet of the polypropylene production plant.

cles. The plant has available two feedstocks, C_3H_6 chemical grade (CG, ~95% propylene) and C_3H_6 refinery grade (RG, ~79% propylene, which requires purification through distillation). As seen in Fig. 2, the refinery grade feedstock is mixed with a fraction of the reactor effluent; this stream must be purified in the distillation column from which the overhead (propylene composition higher than 91%) is mixed with the chemical grade feedstock, and blended with the remaining of the reactor effluent to obtain the proper inlet composition to the polymerization reactor (rich in propylene, usually greater than 80%). Although the chemical grade is considerably more expensive, maximizing the amount of refinery grade may not necessarily be the best economic option. This is because increasing the amount of RG also increases the load in the distillation unit, which in turn compromises the required purity of the propylene feed to the reactor.

The plant of interest produces only homopolymers. Downstream of the reaction area, the produced polymer and various additives (antioxidants, nucleating agents, vis-breaking agents, etc.) are supplied to an extruder so that a given set of reactor targets may be used to generate several final pelletized products, which differ only in the type and quality of the additives. Thus, products with the same (or similar) reactor powder quality targets are grouped into families. Besides, a simple product slate with a pre-optimized order of products in the production wheel is considered. Nearly all consecutive product grades in the wheel have overlapping specifications. While there is a large part of the product wheel with no off-spec production, we assume that gaps where the specifications do not overlap are effectively handled by inserting controlled rhe-

ology grades to cover the amount of transition needed between the prime grades.

Based on the above process description, the multiproduct feedstock optimization problem addressed in this paper can be stated as follows. Given a sequence of polypropylene product grades and their demands to be produced in a finite time horizon H , determine: (a) the production rates for each product, (b) the flowrates and compositions of each stream including feedstocks, and (c) the catalyst flow to the reactor. The objective is to maximize the overall profit such that all the process constraints are satisfied.

Two different multi-product operating scenarios are analyzed: (i) when plans are known, meaning that a fixed demand must be satisfied for each product. In this case, because the total income from sales can be calculated *a priori*, the profit is mainly determined by the feedstock costs, which depend on the balance of chemical and refinery grade used for each product. Alternatively, the scenario (ii) is to consider a fixed plan but to allow some extra production at the end of the schedule. In this case, an additional income can be obtained based on the volume and operating conditions for the extra production selected by the model. For both scenarios the goal is to maximize the profit by finding the optimal feedstocks balance and optimal operating conditions (stream flowrates, production rates, etc.) for the whole schedule.

The main assumptions for the proposed model are as follows:

1. Chemical and refinery grades are purchased from the market at fixed compositions (e.g. 95% and 79%, respectively).

2. Production planning must account for feedstock capacity limits given as maximum rates for the volume of chemical and refinery grade.
3. The distillation process is restricted to the separation of propane-propylene. Reflux rate, pressure, and composition at the bottoms are fixed considering a minimum propylene composition at the distillation overhead.
4. To model the performance of the distillation column, a special adjustment of the effective column equilibrium is made. Further details are presented in [Appendix A](#).
5. Product-families are considered in which products with similar grades are grouped. The product families differ in molecular weight average (M_n , M_w), molecular weight distribution (MWD), and crystallinity.
6. A simplified nonlinear Ziegler-Natta catalytic polymerization model is used to describe the reactor. Fixed parameters characterize the kinetics of the catalyst used, such that each product or product family has characteristic values for the parameters.
7. A minimum propylene composition of the polymerization reactor feed and maximum capacity for the catalyst flow are given.
8. For most of the product wheel, consecutive grades feature overlapping specifications. If this condition does not hold, the schedule includes a specific controlled rheology grade inserted to account for the transition.

3. Mathematical formulations

3.1. Single product model

A nonlinear programming (NLP) formulation is developed first for the single product representation of the polypropylene production problem. The model seeks the best operating conditions to produce a single product grade p . Later, in Section 4, the subscript p is used to refer not only to a single product but also to a family of products with the same reactor powder quality targets. We consider a set of components i (A and B, for propylene and propane, respectively) and a set of flow streams s (RG, CG, DF, DO, DB, MX, RF, RE, S1, and S2) as seen in [Fig. 2](#). The proposed formulation determines the optimal flowrate of component i in flow stream s ($f_{s,i}$), production rate of polypropylene (R), catalyst flow (κ), and propylene composition in reactor feed and distillation overhead (x_{RF} and x_{DO} , respectively) in order to maximize the profit rate of the plant. A set of variables linking the input with the output for the distillation unit (gas and liquid inlets and outlets, absorption and stripping factors, etc.) and the polymerization reactor (weight fraction of propylene in the reactor, slurry density, etc.) are also included. The parameters, such as costs, prices, production limits, kinetic constants, distillation operation conditions (pressure, number of trays, etc.) are assumed to be given.

3.1.1. General flowsheet variables and constraints

Basic constraints to model the flowrate and composition of each stream are presented first. The flowrate of component i on stream s is given by the variable $f_{s,i}$, and the total flowrate F_s is defined by Eq. (1). Eq. (2) defines lower and upper bounds for total flows. Also, fixed compositions are defined by Eq. (3), and upper/lower bounds for compositions are specified by Eqs. (4) and (5).

$$F_s = \sum_{i \in I} f_{s,i} \quad \forall s \in S \quad (1)$$

$$\phi_s^{\min} \leq F_s \leq \phi_s^{\max} \quad \forall s \in S \quad (2)$$

$$f_{s,i} = \sigma_{s,i} F_s \quad \forall i \in I_s^{eq}, s \in S \quad (3)$$

$$\sigma_{s,i}^{\min} F_s \leq f_{s,i} \leq \sigma_{s,i}^{\max} F_s \quad \forall i \in I_s^{lb}, s \in S \quad (4)$$

$$f_{s,i} \leq \sigma_{s,i}^{\max} F_s \quad \forall i \in I_s^{up}, s \in S \quad (5)$$

Some general constraints for mixers and splitters are specified. On the one hand, Eq. (6) corresponds to the mass balance constraints that apply to every mixer or splitter q .

$$\sum_{s \in S_{q,in}} f_{s,i} = \sum_{s \in S_{q,out}} f_{s,i} \quad \forall q \in (MX \cup SP), i \in I \quad (6)$$

On the other hand, composition constraints for splitters are indicated by Eq. (7).

$$f_{s,i}(F_{s'}) = f_{s',i}(F_s) \quad \forall s' \in S_{q,in}, s \in S_{q,out}, i \in I, q \in SP \quad (7)$$

In order to generalize the formulation we define the matrix Q with column vectors $Q_s = [f_{s,A}, f_{s,B}, F_s]^T$ for every stream s . Thus, we denote $STRM(Q)$ as the set of Eqs. (1)–(7) that includes general constraints for all streams.

3.1.2. Simplified distillation process model

To represent the distillation process, we first considered a simple linear correlation based on plant data. This correlation, given by Eq. (8), relates the distillation overhead propylene composition with the inlet flow of propane, and is limited to a restricted operating region. A second degree of freedom of the distillation unit is specified by fixing the composition of the bottoms. Additionally, mass balance constraints for the distillation unit are given by Eq. (9).

$$x_{DO} = \frac{f_{DO,A}}{F_{DO}} = \theta_1 + \theta_2 f_{DF,B} \quad (8)$$

$$f_{DF,i} = f_{DO,i} + f_{DB,i} \quad \forall i \in I \quad (9)$$

3.1.3. Group based distillation model

In order to improve the accuracy of the distillation column representation, we consider a nonlinear shortcut model. Several shortcut models have been proposed in order to describe the mass and energy transfer with few variables and equations ([Kremser, 1930](#); [Fenske, 1932](#); [Gilliland, 1940](#)). Recent short-cut models have been reported by [Bagajewicz and Manousiouthakis \(1992\)](#), [Bausa et al. \(1998\)](#) and [Caballero and Grossmann \(1999\)](#).

Group methods have been proposed, on the one hand to overcome the size and complexity of tray-by-tray models, and on the other hand to address accuracy and flexibility in the application of shortcut models in simulation and optimization. Group methods aggregate sections of stages in the distillation column ([Kremser, 1930](#)) as shown in [Fig. 3](#). The specifications for the vapor and liquid inlet (V_{N+1} and L_0 , respectively) serve as fixed inputs to the model, which are used to approximate the outlet stream properties, such as temperature, flow and composition (V_1 and L_N for the vapor and liquid, respectively). In this paper we use the aggregated group-based method of [Kamath et al. \(2010\)](#), which is an extension of Kremser's model where the inputs of the model are specified (vapor V_{N+1} and liquid L_0), to predict the vapor and liquid outputs (V_1 , L_N , respectively) in terms of the cascade specifications. Additionally, adiabatic operation and pressure drop in the cascade are considered.

The equations of [Kamath et al. \(2010\)](#) include mass and energy balances (Eqs. (10) and (11)) and the general performance of the cascade (Eq. (12)). Recovery factors for absorption and stripping are given by Eq. (13). The effective absorption and stripping factors are represented by average values for all trays in the cascade (Eq. (14)). Eq. (14) uses absorption and stripping factors at the top and bottom of the cascade, calculated using Eq. (15). The outlet vapor and liquid are constrained to be at their dew and bubble point conditions (Eqs.

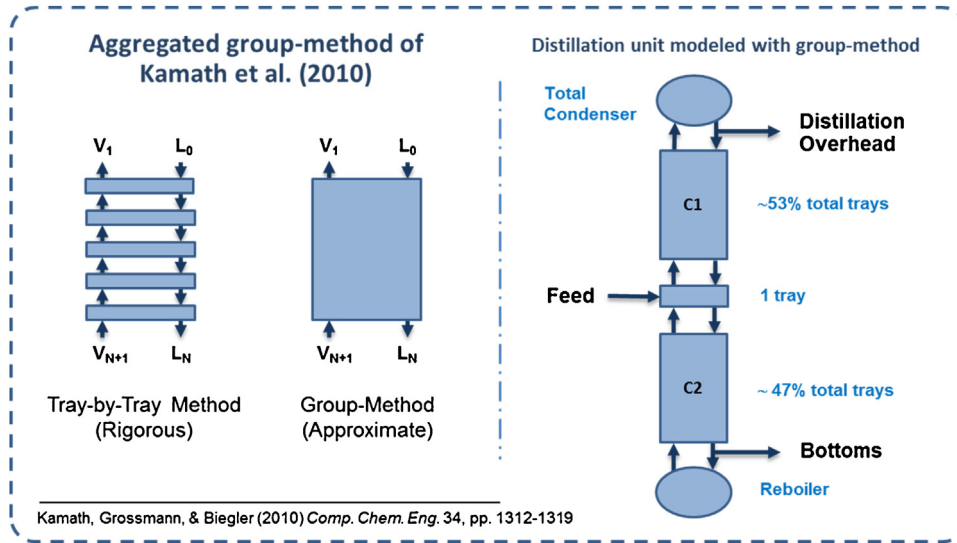


Fig. 3. Aggregated group method of Kamath et al. (2010).

(16) and (17)), respectively. Finally, the model approximates the overall mass balance of the cascade with Eq. (18). For a detailed explanation of the model, see Kamath et al. (2010).

$$V_{N+1,i} + L_{0,i} = V_{1,i} + L_{N,i} \quad \forall i \in I \quad (10)$$

$$\sum_{i \in I} (V_{N+1,i} H_{N+1,i}^V + L_{0,i} H_{0,i}^L) = \sum_{i \in I} (V_{1,i} H_{1,i}^V + L_{N,i} H_{N,i}^L) \quad (11)$$

$$V_{1,i} = V_{N+1,i} \phi_{A,i} + L_{0,i} (1 - \phi_{S,i}) \quad \forall i \in I \quad (12)$$

$$\phi_{A,i} = \frac{A_{e,i} - 1}{(A_{e,i})^{N+1} - 1}; \quad \phi_{S,i} = \frac{S_{e,i} - 1}{(S_{e,i})^{N+1} - 1} \quad \forall i \in I \quad (13)$$

$$A_{e,i} = [A_{N,i} (A_{1,i} + 1) + 0.25]^{0.5} - 0.5; \quad (14)$$

$$S_{e,i} = [S_{N,i} (S_{1,i} + 1) + 0.25]^{0.5} - 0.5 \quad \forall i \in I$$

$$A_{1,i} = \frac{L_1}{K_{1,i} V_1}; \quad A_{N,i} = \frac{L_N}{K_{N,i} V_N}; \quad (15)$$

$$S_{1,i} = \frac{1}{A_{1,i}}; \quad S_{N,i} = \frac{1}{A_{N,i}} \quad \forall i \in I$$

$$\sum_{i \in I} \frac{y_{1,i}}{K_{1,i}} = 1 \quad (16)$$

$$\sum_{i \in I} K_{N,i} x_{N,i} = 1 \quad (17)$$

$$L_1 - L_N \approx V_1 - V_N \quad (18)$$

Variables V_1 and L_N in Eqs. (15) and (18) are defined as follows:

$$V_1 = \sum_{i \in I} V_{1,i}; \quad L_N = \sum_{i \in I} L_{N,i}$$

Also, the new variables L_1 and V_N are introduced to represent the cascade of trays. In Eqs. (16) and (17) the compositions $y_{1,i} = V_{1,i}/V_1$ and $x_{N,i} = L_{N,i}/L_N$ are used. The Antoine's equation with a specific set of effective parameters has been used to calculate the saturation pressure of each component i ($P_{j,i}^0$) as a function of temperature (t_j), and the corresponding $K_{j,i} = P_{j,i}^0/P_j$ value (with $j = 1$ or N , and $i \in I$), considering ideal behavior of the mixture (see Appendix A).

In order to generalize the formulation for a single cascade, we define the matrix,

$$\mu = \begin{bmatrix} \eta_A & \eta_B \\ L_1 & V_N \end{bmatrix} \quad (19)$$

where each vector η_i includes all the variables related to component i :

$$\eta_i = [L_{0,i}, V_{1,i}, L_{N,i}, V_{N+1,i}, A_{1,i}, A_{N,i}, A_{e,i}, S_{1,i}, S_{N,i}, S_{e,i}, \phi_{A,i}, \phi_{S,i}]^T \quad \forall i \in I \quad (20)$$

Using μ we define $CTRAYS(\mu)$ as the set of constraints (10)–(20). Thus, to represent the distillation unit we introduce,

$$\mu_c = \begin{bmatrix} \eta_A^c & \eta_B^c \\ L_1^c & V_N^c \end{bmatrix}, \quad (21)$$

where:

$$\eta_i^c = [L_{0,i}^c, V_{1,i}^c, L_{N,i}^c, V_{N+1,i}^c, A_{1,i}^c, A_{N,i}^c, A_{e,i}^c, S_{1,i}^c, S_{N,i}^c, S_{e,i}^c, \phi_{A,i}^c, \phi_{S,i}^c]^T \quad \forall i \in I, c \in \{C1, C2\} \quad (22)$$

Also, we define,

$$\mu_{c,j} = \begin{bmatrix} L_{j,A}^c & L_{j,B}^c \\ V_{j+1,A}^c & V_{j+1,B}^c \end{bmatrix}, \quad (23)$$

as a sub-matrix of μ_c with all the vapor and liquid flowrates, leaving or entering (respectively), the tray $j + 1$ of cascade c . Thus, either $j = 0$ is used to refer to the interface at the top of the cascade, or $j = N$ is used to reference the bottom.

Finally, given $U = [\mu_{C1}, \mu_{C2}]$, Eq. (24) defines the set of constraints needed to model the distillation process by means of the aggregated group method of Kamath et al. (2010).

$$\begin{aligned} DESTN(Q, U) = \\ U = [\mu_{C1}, \mu_{C2}] \\ CTRAYS(\mu_c), \forall c \in \{C1, C2\} \\ FEED(Q_{DF}, \mu_{C1,N}, \mu_{C2,O}) \\ TCOND(\mu_{C1,O}, Q_{DO}) \\ REBL(\mu_{C2,N}, Q_{DB}) \end{aligned} \quad (24)$$

Additional constraints modelling the feed tray, total condenser, and partial reboiler (Fig. 2) are required, including mass/energy balances and vapor-liquid equilibrium relations. Since a total condenser is used, the distillation overhead propylene composition defined by $TCOND(\mu_{C1,O}, Q_{DO})$ is equivalent to:

$$x_{DO} = \frac{f_{DO,A}}{F_{DO}} = \frac{V_{1,A}^{C1}}{V_1^{C1}} \quad (25)$$

3.1.4. Group based model vs. linear correlation

Fig. 4 shows the distillation column behavior using both the linear correlation and the group based model representation. For the later, a fixed reflux rate and composition of the bottom are used. The horizontal axis of Fig. 4 represents the volume of propane fed to the column, independently of the total feed (propane + propylene). On the one hand, the linear correlation shown in Fig. 4 maps the amount of propane that enters the splitter with the corresponding propane composition at the top (vertical axis). Thus, it applies to any feed composition. On the other hand, the results of the group-based method depend on the feed composition. To analyze the behavior of this approximate model, three different feed compositions were tested (22%, 24%, and 26% weight). For each composition, as shown in Fig. 4, the group-based representation has been solved using 36 fixed feed flowrates, and the overhead propane composition has been obtained. Three flowrates are indicated as reference points: (a) the maximum feed flowrate, (b) half of the maximum, and (c) the maximum plus an additional 20% feed flow.

We can observe that, for each feed composition tested, in some range the linear correlation and group based model predict similar behavior of the distillation column. However, out of this range the predictions made by the linear correlation are quite different and, in some points, even unrealistic. The empirical model (linear correlation) involves a smaller and more tractable model, but loses accuracy out of certain operating region. In contrast, the group-based model provides flexibility to optimize the distillation column under multiple feed flowrates and compositions, providing a good approximation without requiring a tray-by-tray model.

3.1.5. Polymerization reaction model

The polymerization reactor is the key unit of the process being considered. A kinetic model relating catalyst flow, catalyst yield, and input flow (propylene and propane usually with 80–20 ratio, respectively) is used. The reactor feed is converted into different grades of polypropylene (depending on the product recipe) and a reactor effluent with the remaining components (monomer recovered for recycle, usually 60% propylene) as seen in Fig. 5.

The plant produces only homopolymers so the quality parameters targeted for a given product grade (or family) are XS% (xylene soluble fraction, which relates to isotacticity, crystallinity) and MFI (melt flow index, which relates to molecular weight). While the average molecular weight may be obtained through analytical methods such as Size Exclusion Chromatography (SEC) or Gel Permeation Chromatography (GPC), these are costly and time-consuming as a plant lab quality control. Instead, a simpler and quicker test (MFI) is employed as a measure correlated to molecular weight (see Fig. 6a).

The process main regulating agents are hydrogen (primarily for molecular weight control) and electron donor (primarily for crystallinity control). A cocatalyst, typically an aluminum alkyl, is also employed. The chain transfer agent used for polypropylene is hydrogen and the molecular weight of the polymer is strongly correlated to chain transfer agent concentration. Hydrogen also has a profound effect on the catalyst activity due to its ability to reactivate dormant sites – in general, products with low MFI (low H_2 concentration) require a larger amount of catalyst to achieve the same production rate as products with high MFI (high H_2 concentration). The effect of hydrogen and electron donor as regulating agents of

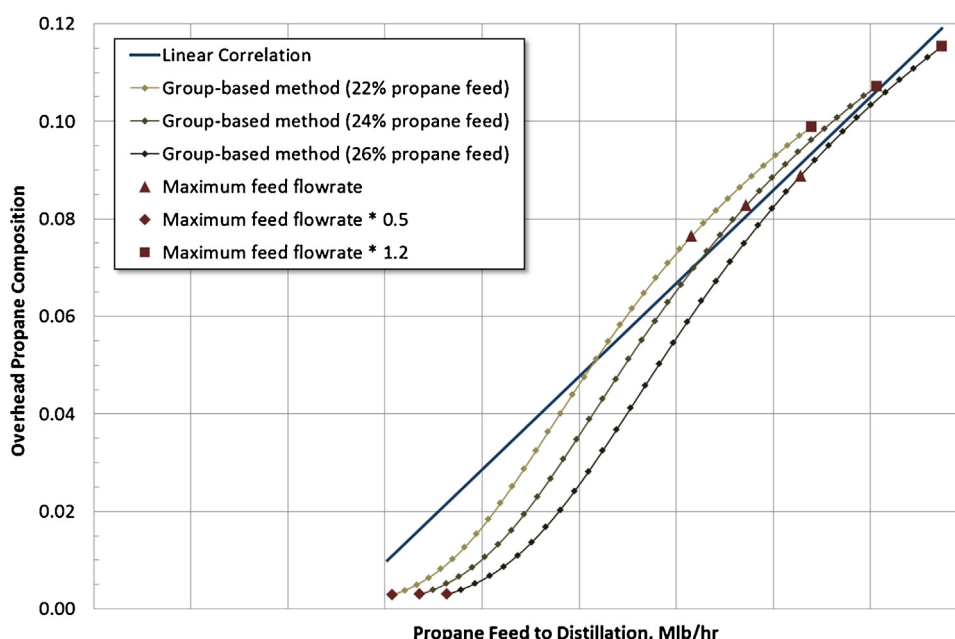


Fig. 4. Comparison of distillation performance: group based method vs. linear correlation.

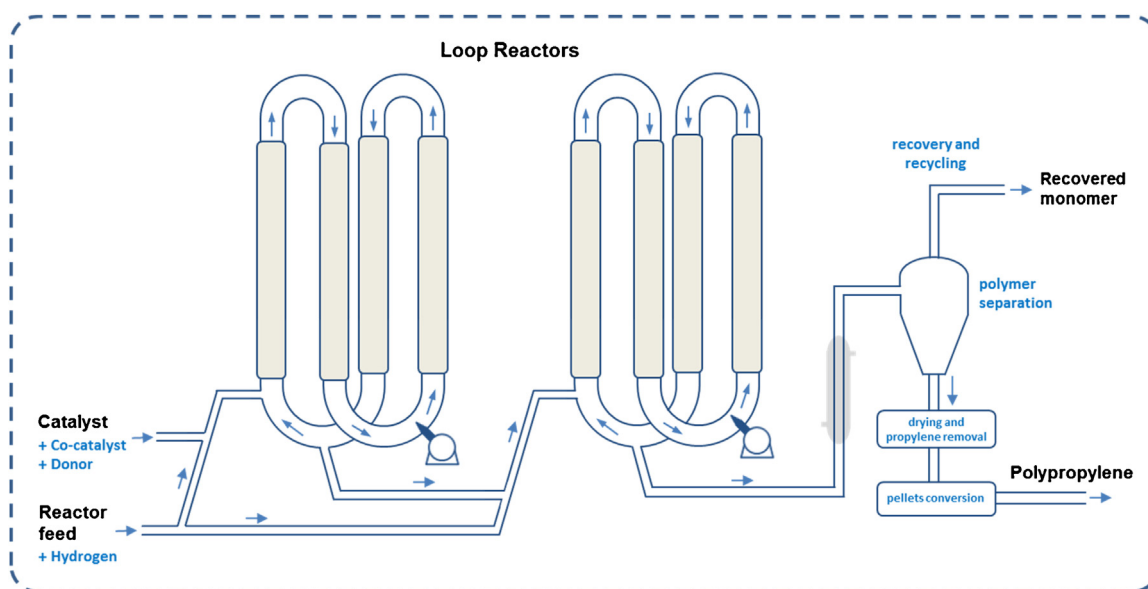
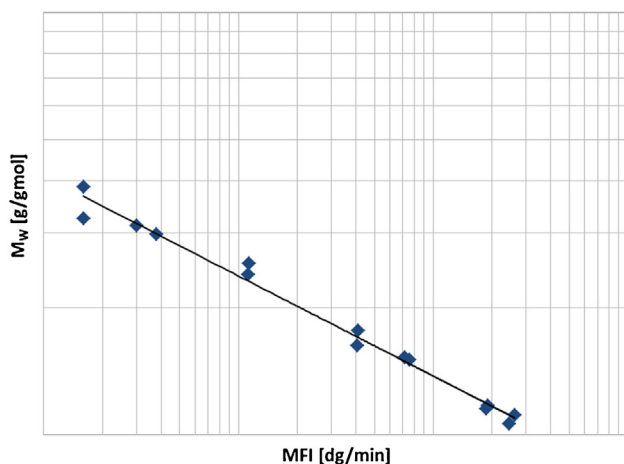
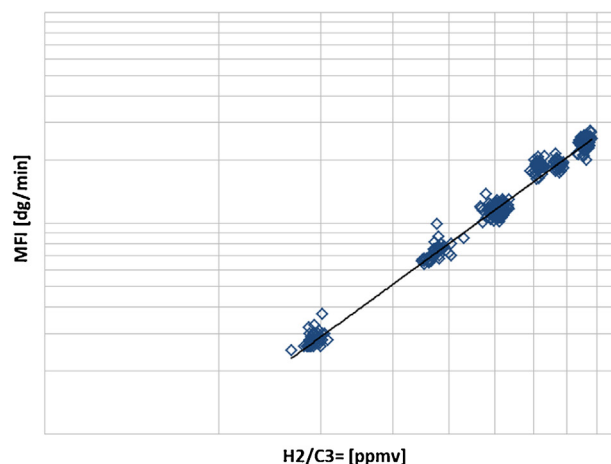


Fig. 5. Double-loop polymerization reactor scheme.

a) Weight Average Molecular Weight to MFI

b) MFI to H₂/monomer ratioFig. 6. a) Polypropylene weight average molecular weight as a function of MFI, b) Example of melt flow index (MFI) correlated with H₂ to monomer ratio for a given type of catalyst, cocatalyst, and donor.

Ziegler-Natta-catalyzed propylene polymerization is supported by several experimental studies, e.g. Al-haj Ali et al. (2006) and Garoff et al. (2003). A rigorous kinetic model would consider separate effects of initiation, propagation, chain transfer to hydrogen, chain transfer to monomer, various types of deactivation, reactivation with hydrogen, etc.; with an activation energy for each reaction, and a complete set of reaction constants for each type of site considered. However, this type of formulation would be overly complex for the purpose of the present study.

A simplified nonlinear Ziegler-Natta catalytic polymerization model describing the reactor has been considered. The main assumptions are: (1) the polymerization rate is proportional to both monomer concentration and number of active catalyst sites; (2) the number of active catalyst sites decays at a rate proportional to the current number of sites; and (3) for simplicity a single site model is used.

For each product grade p , the product recipe includes the type of catalyst, cocatalyst, and donor. The feed of hydrogen, electron

donor, and cocatalyst are set in the recipe as ratios, for example, “aluminum alkyl to propylene”, “aluminum alkyl to electron donor”, and “hydrogen to propylene”. These ratios are the same for all products within a family. By using ratios, the same recipe applies to a wide range of production rates (i.e., recipes do not change based on production rate). An example of the correlation between MFI and H₂ to monomer ratio for a given type of catalyst, cocatalyst, and donor is shown in Fig. 6b.

Using this approach, the simplified kinetic model considers only monomer feed composition and catalyst rate as inlet decision variables, while the other feeds are fixed (via ratios) to maintain the product quality at different production rates. The effect of hydrogen, donor, and cocatalyst are lumped into the propagation (K_p) and deactivation (KD_p) constants, which are different for each product family. Simplified kinetic models with kinetic parameters obtained from quantitative experimental data have been developed by Matos et al. (2001), Matos et al. (2002), and Al-haj Ali et al. (2006), among others. Moreover, the described use of a recipe wherein certain

feed ratios are fixed to deliver desired product targets (related to crystallinity and molecular weight) is common in the industry.

Eq. (26) relates the production rate to the catalyst flow and yield, where R represents the total loop production rate (lb PP/h); R_1 and R_2 are the production rates in each loop (lb PP/h); Y_1 , Y_2 are the catalyst yields in each loop (lb PP/lb catalyst); and κ is the catalyst flow (lb catalyst/h).

Eq. (27) describes the catalyst yield in loop n based on the monomer concentration (x_n) and residence time (τ_n), multiplied by the kinetic rate constant K_p . The definition of K_p , given in Eq. (28), encompasses a propagation rate constant (K_p^0) and the initial number of active catalyst sites/lb catalyst (C_0). The propagation rate constant $K_p^0 = K_p^0(T, TEA, Donor, H_2)$ [lb PP/(lb catalyst · hr · monomer mass fraction)] is a lumped term that combines all the individual elementary reactions of initiation, catalyst, cocatalyst (TEA = triethylaluminum), donor, hydrogen effects, chain transfer, etc. into one “effective” propagation rate. It also has an Arrhenius temperature dependence. For unimodal loop operation, it is assumed that conditions are similar in both reactors so K_p is the same for both loops.

Eq. (27) also considers the deactivation, which is assumed to be a first order process proportional to the number of catalyst sites. The deactivation constant $KD_p = KD_p(T, TEA, Donor, H_2)$ is affected by hydrogen, temperature, donor, etc., and an average value is used on the model.

A product or product family, for a given catalyst and donor type, is defined by its crystallinity and MFI targets. Values of K_p and KD_p have been obtained from plant data.

$$R = R_1 + R_2 = (Y_1 + Y_2) \cdot \kappa \quad (26)$$

$$Y_n = \frac{K_p x_n \tau_n}{\prod_{m=1}^n (1 + KD_p \tau_m)} \quad n = 1, 2 \quad (27)$$

$$K_p = K_p^0 C_0 \quad \forall p \in P \quad (28)$$

$$K_p = K_p^0 C_0 \quad \forall p \in P \quad (28)$$

Constraints (29)–(31) define bounds for the production rate, the catalyst flow and the total catalyst yield. Notice that the bounds in Eq. (29) depend on the product grade p being produced.

$$R_p^{\min} \leq R \leq R_p^{\max} \quad (29)$$

$$\kappa \leq \kappa^{\max} \quad (30)$$

$$Y_1 + Y_2 \geq Y^{\min} \quad (31)$$

Eq. (32) defines the solids fraction (polypropylene) in the outlet of loop n (w_n). For the homopolymer line under study, the density of solids $\rho_S = 900 \text{ kg/m}^3$ and the slurry density ρ_{SL} are fixed parameters, while the density of liquids in each loop n ($\rho_{L,n}$) is a variable to be determined by the model. A non-ideal mixing behavior, as a result of centrifugal forces caused by high-speed circulation, is accounted for by including a fixed discharge factor $\beta_n \geq 1$ (see Reginato et al., 2003). The estimation $\beta_n = (1 + \varphi)$ is used in the model, where the centrifugation fraction φ is defined as the ratio between the apparent recycle flow and the total effluent from the reactor (including solids), based on plant data.

$$w_n = \frac{\beta_n \rho_S (\rho_{SL} - \rho_{L,n})}{\rho_{SL} (\rho_S - \rho_{L,n})} \quad n = 1, 2 \quad (32)$$

For each loop n , Eq. (33) defines the weight fraction of propylene in the reactor slurry (x_n) as the quotient between the propylene in the slurry (i.e., propylene feed composition minus output solids fraction) and the fraction of liquids in the slurry.

$$x_n = \frac{x_{RF} - w_n}{1 - w_n} \quad n = 1, 2 \quad (33)$$

In Eq. (33) the reactor feed propylene composition is given by $x_{RF} = \frac{f_{RF,A}}{f_{RF}}$. Besides, at each loop n the monomer concentration (x_n) is associated to the density of liquids ($\rho_{L,n}$) by:

$$\rho_{L,n} \left(\frac{x_n}{\rho_A} + \frac{1 - x_n}{\rho_B} \right) = 1 \quad n = 1, 2 \quad (34)$$

Eq. (35) defines the weight of solids (i.e., polypropylene) produced at loop n during time τ_n , assuming steady state operation, based on the loop volume, the slurry density, and the solids fraction. Notice that the residence time τ_n can be derived from this equation.

$$\tau_n \left(\sum_{m=1}^n R_m \right) = V \rho_{SL} w_n \quad n = 1, 2 \quad (35)$$

Finally, assuming ideal CSTR behavior, Eq. (36) defines the propylene composition of the reactor effluent, and Eq. (37) defines the material balance constraints for the whole polymerization process.

$$f_{RE,A} = x_2 f_{RE} \quad (36)$$

$$\begin{bmatrix} f_{RF,A} \\ f_{RF,B} \end{bmatrix} = \begin{bmatrix} R + f_{RE,A} \\ f_{RE,B} \end{bmatrix} \quad (37)$$

In order to generalize the formulation we define the matrix $V = [v_1, v_2]$, where each vector v_n includes all the variables related to loop n :

$$v_n = [Y_n, R_n, x_n, \tau_n, w_n, \rho_{L,n}]^T \quad n = 1, 2 \quad (38)$$

Finally, the set of constraints (26)–(38) is denoted as $POLYM_p(Q, V, \kappa, R)$, where the subindex p determines the product grade (or family) being targeted by selecting the parameters K_p , KD_p , R_p^{\min} , and R_p^{\max} included in Eqs. (27)–(29).

3.1.6. Objective function

Eq. (39) defines for a single product (or product family) p the profit rate (\$/h) of the plant in steady state operation. The profit rate includes the sales rate obtained from the production rate R (lb/h) and the sales price of the polypropylene produced (\$/lb), plus an average return value per hour obtained by selling back the distillation bottoms to the provider (r_{DB} : return price of distillation bottoms, \$/lb), and minus the cost rate of the feedstocks and catalyst used, where the costs c_{RG} , c_{CG} , and $c_p^{catalyst}$ are also given in \$/lb, and the flowrates in lb/h.

$$PROFR_p(Q, \kappa, R) = \text{price}_p R + r_{DB} F_{DB} - \left(\sum_{s \in \{RG, CG\}} c_s F_s \right) - c_p^{catalyst} \kappa \quad (39)$$

Using Eq. (39) the single product mathematical model (40) is presented, where the profit rate is maximized to obtain the optimal plant throughput for product p . Upper and lower bounds for all model variables are represented by the domain Ω .

$$\begin{aligned} &\text{Maximize} && PROFR_p(Q, \kappa, R) \\ &\text{s.t.} && STRM(Q) \\ &&& DESTN(Q, U) \\ &&& POLYM_p(Q, V, \kappa, R) \\ &&& (Q, U, V, \kappa, R) \in \Omega \end{aligned} \quad (40)$$

Notice that neither a product demand nor a production horizon is considered in the single product formulation (40). These

are handled by the multiple-product model presented in the next section.

Finally, an alternative objective function (41), maximizing the production rate, can be considered for the single product model, which is equivalent to minimizing the production time.

$$\text{Maximize } R \quad (41)$$

3.2. Multiple-product formulation

3.2.1. Model extension to handle multiple products

The model presented in Section 3.1 is generalized to consider the case where, instead of a single product, a sequence of products with fixed demands is being produced. To this end, the production schedule is specified by means of consecutive time slots $k \in K$, where a product grade $p(k)$ is assigned to each slot k . The end product $p(k)$ is therefore produced by the polymerization reactor at slot k .

The multiple-product feedstock optimization model is presented in Eq. (42). The objective function (42.1) represents the overall profit to be maximized, where $PROFR_{p(k)}$ is the profit rate as in Eq. (39) and T_k is a new continuous variable that represents the actual time allotted to produce product $p(k)$ at slot k . Note that the profit rate (\$/h) is now multiplied by the production time (hr). The constraints for the stream compositions and material balances (STRM), the aggregated group based distillation model (DESTN), and the polymerization reactor ($POLYM_{p(k)}$), as defined in Section 3.1, are all applied for each time slot k . Besides, production demands are enforced by Eq. (42.5), where R^k is the production rate of polypropylene at slot k and d_k is the demand of product $p(k)$. Finally, Eq. (42.6) ensures that a specified time horizon H is not exceeded.

$$\text{Maximize } \sum_{k \in K} T_k \cdot PROFR_{p(k)}(Q^k, \kappa^k, R^k) \quad (42.1)$$

$$\text{s.t. } STRM(Q^k) \quad \forall k \in K \quad (42.2)$$

$$DESTN(Q^k, U^k) \quad \forall k \in K \quad (42.3)$$

$$POLYM_{p(k)}(Q^k, V^k, \kappa^k, R^k) \quad \forall k \in K \quad (42.4)$$

$$T_k \cdot R^k = d_k \quad \forall k \in K \quad (42.5)$$

$$\sum_{k \in K} T_k \leq H \quad (42.6)$$

$$(Q^k, U^k, V^k, \kappa^k, R^k) \in \Omega \quad \forall k \in K$$

$$T_k \in [0, H] \quad \forall k \in K$$

Note that the above slot-based NLP scheduling model does not include sequencing decisions since a fixed sequence of products is specified. Besides, due to assumption 8 (see Section 2) sequence dependent transition times and costs are not considered.

The objective function (42.1) can be simplified using Eq. (39):

$$T_k \cdot PROFR_{p(k)}(Q^k, \kappa^k, R^k) = price_{p(k)} d_k + \left(r_{DB} F_{DB}^k - \sum_{s \in \{RG, CG\}} c_s F_s^k \right) T_k - c_{p(k)}^{catalyst} (\kappa^k T_k) \quad (43)$$

In Eq. (43) the polypropylene sales income at slot k is a constant value, while the remaining terms correspond to the extra income from sales of an intermediate product (DB, distillation bottoms) and the acquisition cost of both the feedstocks (refinery and chemical grade) and the catalyst used.

An alternative objective function is given by Eq. (44), where the total production time or makespan is minimized.

$$\text{Minimize } MK = \sum_{k \in K} T_k \quad (44)$$

3.2.2. Handling extra production

In Eq. (44) time is a variable to be optimized in the sense that a given slate can either be run at maximum rate (i.e. until some constraint is hit) and finish in time t_1 or be run slower (for example, taking a higher proportion of RGP vs CGP) and finish in time t_2 , which will be larger than t_1 . The high production rate scenario may require more CGP and have a higher feedstock cost, but there would be “extra” time ($t_2 - t_1$) compared to the low production rate scenario. This extra time can be used for additional production. For instance, if the plant is sold out, the extra production can be considered to be worth the average unit contribution margin (UCM) of the annualized production (in other words, over the course of the year, the plant would like to make a little more of all products).

In order to assess the possible gain of having some extra production, an additional time slot k^+ is introduced at the end of the schedule and associated with an average ‘slack’ product p^+ . Since there is no fixed demand, the volume of slack product produced (if any) is determined by the model but limited to a given maximum. To handle the extra production only two changes are needed on the multi-product feedstock optimization model: 1) for $k = k^+$ replace the parameter d_k in Eq. (43) with the term $(T_k \cdot R^k)$; and 2) exclude the constraint (42.5) for time slot k^+ replacing it by the upper bound indicated by Eq. (45).

$$T_{k^+} \cdot R^{k^+} \leq SL^{\max} \quad (45)$$

4. Solution strategy

In order to outline the solution strategy for the single and multiple product formulations presented in Section 3, three alternative models are defined. Model 1 is the single product formulation given by Eq. (40), where the problem goal is the maximization of the profit rate. Model 2 is the multiproduct model given by Eq. (42) which is solved to maximize the overall profit for a given schedule of products. Finally, Model 3 is the multiproduct formulation extended to consider a ‘slack’ product at the end of the schedule. This model provides demand information for the extra production scenario, while also maximizing the overall profit (see Section 3.2.2).

Since the proposed formulations involve nonlinearities, ‘good’ initial solutions are required in order to provide a starting point for the NLP solver and obtain optimal, or even feasible, solutions. An accumulative approach of solving each model starting with an initial solution obtained from the previous models is used. The solution strategy for each case is explained next.

4.1. Single-product model

The main techniques used to help the solver find feasible solutions are: i) initializing variables, ii) providing upper and lower bounds for all variables (mostly the ones included in bilinear terms), and iii) scaling the variables and constraints. A two-step approach is applied to solve model 1. First, the simplified representation of the distillation column given by Eqs. (8) and (9) is used instead of the set of constraints $DESTN(Q, U)$ defined in Eq. (24). An optimal solution is found with this simplified model, which provides feasible values for the production rate, the flowrates/compositions of streams, and the polymerization reactor variables. While it loses accuracy on the distillation column representation, the solution obtained is a good initial solution for the model defined in Eq. (40). As a second step, the single product model (40), including the group-based

representation of the distillation process, is solved. The solution obtained can be used as an initialization point for the multiproduct model (as described in the next section).

4.2. Multiple-product model

The multiple-product feedstock optimization model involves a single product model for each time slot k . Given a schedule with several dozen products, each one allocated to a single slot k , an optimal solution of the multiple-product model could be hard or even impossible to obtain on reasonable CPU times using state-of-the-art NLP solvers.

However, in many scenarios it is possible to reduce the NLP model size by considering aggregated demands. Because they feature the same reactor targets, mainly determined by the kinetic parameters K_p and KD_p , products of the same family have the same production constraints. Therefore, it is possible to aggregate and handle together the demands of products belonging to the same family. This aggregation reduces the number of time slots k by considering only one slot for each family.

Once an aggregated schedule is calculated, and before solving the multiple-product formulation, the single product model is applied to each product family. For these optimizations, the sales price of the family is calculated as the average price of the products belonging to the family, weighted by their demands. The solutions of model 1 are then used to initialize the variables of model 2, providing a ‘good’ initial solution for each time slot k . In particular, feasible values for the variables T_k are derived using Eq. (42.5). Next the model 2 is solved and an optimal (or locally optimal) solution is found. Based on this solution, the operating conditions for each product family can be easily used to derive a detailed production schedule. To this end, aggregated results are disaggregated by considering the solution for each family as the same for all the products belonging to that family (e.g. production rate, feedstock flowrates, etc.). Also, the production time for each product will be proportional to the time allotted to its family, according to the demand.

In summary, the solution methodology used for the multiple-product feedstock optimization model is presented in Fig. 7. The implementation includes an aggregation/disaggregation procedure, which allows obtaining solutions for large schedules by significantly reducing the model size and complexity. Besides, it is critical to have ‘good’ initial solutions, which are obtained from the application of the single product model for each time slot k .

4.3. Accounting for extra production

In this scenario the model includes an additional time slot k^+ at the end of the schedule to account for extra production. In contrast to the multiple-product model where every time slot had a fixed demand, the demand allocated to the slack product p^+ is a variable to be determined by the model. The solution methodology used for model 3 is similar to the one proposed for the multiple-product model, but considering the following adjustments:

First, the single product model is solved for each time slot k (or product family when aggregated demands are used) using the production rate, i.e. objective function (41), instead of the profit rate as the problem goal to be maximized. Since every product operates at its maximum rate, the results of model 1 represent a feasible solution where the plant is operated at its maximum production level. Consequently, the solutions of model 1 can be used to calculate the optimal makespan (MK). If the production campaign finishes before the time horizon limit ($MK < H$), an idle time to allocate more production is available. In this case, the additional time slot k^+ is initialized using the idle time by fixing $T_{k^+} = H - MK$, and the single product model is solved for slot k^+ . The solution includes a feasible production demand of the new (slack) product. In order to generate

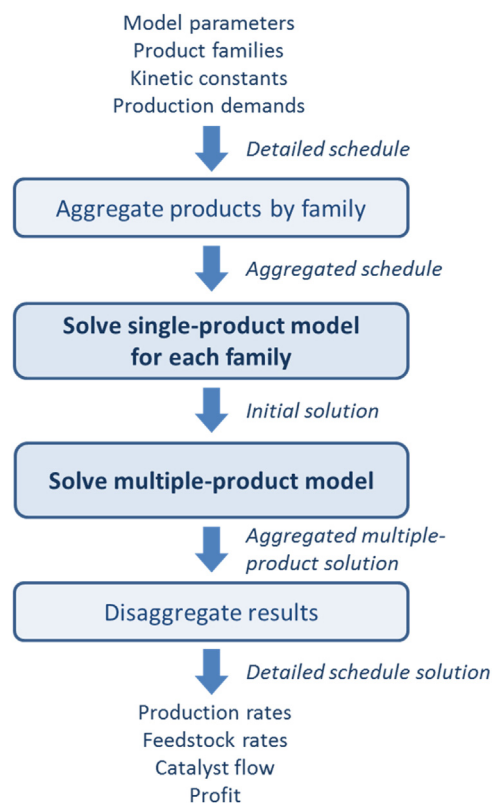


Fig. 7. Solution methodology for the multiple-product problem.

Table 1

Single product model statistics and computational time.

	Single-product model
Variables	157
Constraints	152
Nonlinearities	264
CPU time (s)	1.38 ^a

^a Solver: BARON 15.9 (includes initialization using simplified distillation model).

an initial solution for the multiple-product model 3, the previously fixed time of slot k^+ (T_{k^+}) is freed, and the solutions of the single product models (considering the extra production) are combined. Finally, model 3 is solved using the overall profit as the objective function. In summary, this scenario modifies the production schedule by pushing to operate at the maximum production capacity in order to allocate the new “slack” product before the model is solved.

5. Results and discussion

In this section, results for different test cases applying the single and multiple-product formulations are presented. In order to analyze the performance of the model, the results for the single product scenario are presented first. Afterwards, medium and long term test cases are solved to illustrate the potential economic impact of the proposed method.

The proposed feedstock optimization methodology has been implemented in GAMS 24.5 and solved using state-of-the-art NLP solvers on an Intel® Core™ i7 at 3.2GHz machine. The size and complexity of the proposed models are reported in Tables 1 and 2, in which the number of variables, constraints, and computational times are shown for all the case studies presented in the next sections. On the one hand, Table 1 presents the model statistics and a representative example of the computational time needed to solve model 1. Because it features a small model size, the single-product

Table 2
Model statistics and computational times for multiple-product examples.

Case study	Model	Variables	Constraints	Nonlinearities	CPU time (s)		
					Aggregation/initialization ^a	Multiple-product solution ^b	Total time
Medium term test case	2	937	902	1584	4.98	0.16	5.14
	3	1093	1051	1847	9.31	0.16	9.47
Long term test case	2	1561	1502	2640	9.66	0.18	9.84
	3	1717	1651	2903	12.44	0.14	12.58

^a Overall time of aggregation, initialization of single-product models at each time-slot (BARON 15.9), and disaggregation.

^b Locally optimal solution (CONOPT 3.17).

formulation is efficiently solved to global optimality using BARON (v. 15.9). On the other hand, Table 2 shows the model statistics and computational times for the multiple-product case studies. These examples are solved using the aggregation/disaggregation procedure described in Section 4.2 (for model 2), which is extended in Section 4.3 to account for extra production (model 3). Most of the time needed to solve each multiple-product problem is spent on the initialization step. Here, for each product family, solutions of the single-product model are obtained with BARON and used to build an initial feasible solution for models 2 or 3. Due to their larger size and complexity, the multiple-product models are solved using CONOPT (v. 3.17). As shown in Table 2, the solutions of models 2 and 3 are efficiently obtained in less than 1 s of CPU time, provided the ‘good quality’ of the initial point found with the proposed methodology. While the best solutions always satisfy local optimality conditions, they are not necessarily global solutions. It is important to mention, however, that for almost all the examples analyzed the local solutions obtained with CONOPT were also proven to be global solutions using BARON (with CPU times between 2 and 20 s.) There was only one instance of the long term test case where BARON could not complete the spatial branching search within a time limit of 5 h. (22% relative gap).

Due to confidentiality reasons, for all the test cases presented in the next sections the details on the product prices, production rates, feedrates of RGP and CGP, distillation unit and polymerization reactor parameters and operating conditions, etc., are not provided. Besides, in most tables/figures normalized values are used to give a qualitative idea of the results being analyzed.

5.1. Single product example

The model is first applied to maximize the profit rate (\$/h) for a single product assuming continuous steady state operation. The main system constraints, which apply to the flowsheet presented in Fig. 2, include the following: (i) maximum rates for the refinery grade feedstock (RG), splitter feed (DF), and monomer recycle to distillation (S2), (ii) maximum propane compositions in distillation overhead (DO) and reactor feed (RF), (iii) maximum flow and minimum yield for the catalyst, and (iv) lower and upper bounds for the production rate, which depend on the product family. Distillation column parameters are pressure ~9 atm, total condenser, partial reboiler, single feed, fixed bottoms composition (~5% propylene) and maximum reflux rate.

To analyze the performance of the model, results for two products (P₁ and P₂) belonging to different product families (F₁ and F₂) are presented. In particular, product P₁ is a low MFI product, and P₂ is a high MFI product. In this example, feedstock prices are given by a PGP marker of 0.68 \$/lb, a CGP to PGP spread of 1.5 cpp (cents per pound), and a RGP-PGP spread of 12 cpp. For each product the model is solved considering the following three fixed production rates: (a) the minimum rate, (b) an average between the maximum and minimum rates, and (c) the maximum production rate. If not fixed, the optimal solution usually drives the production to the maximum rate while balancing the feedstocks (RGP vs. CGP)

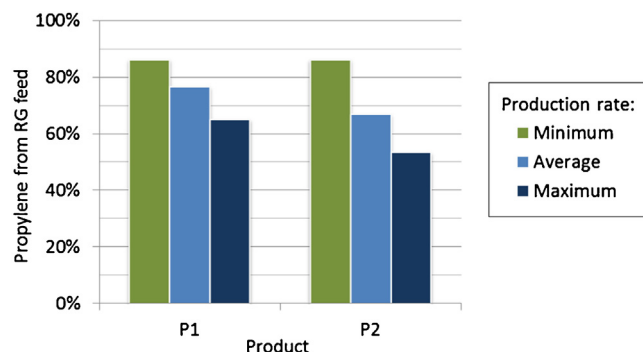


Fig. 8. Propylene sourced from RGP for products P₁ and P₂ at different production rates.

needed in order to minimize the total cost. The goal of forcing certain production rates is to understand how the other constraints on the system, including limitations inherent to the kinetics of the products (characterized by the K_p and KD_p parameters), impose limits on the plant operating conditions and selected feedstock types.

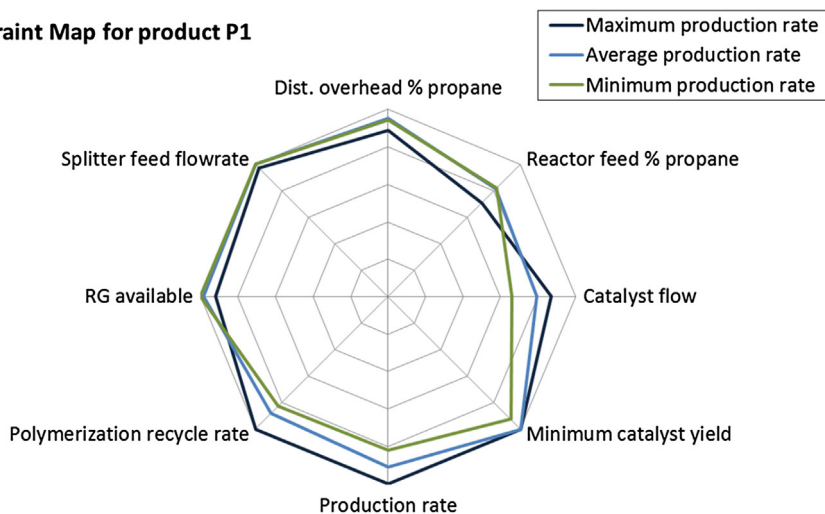
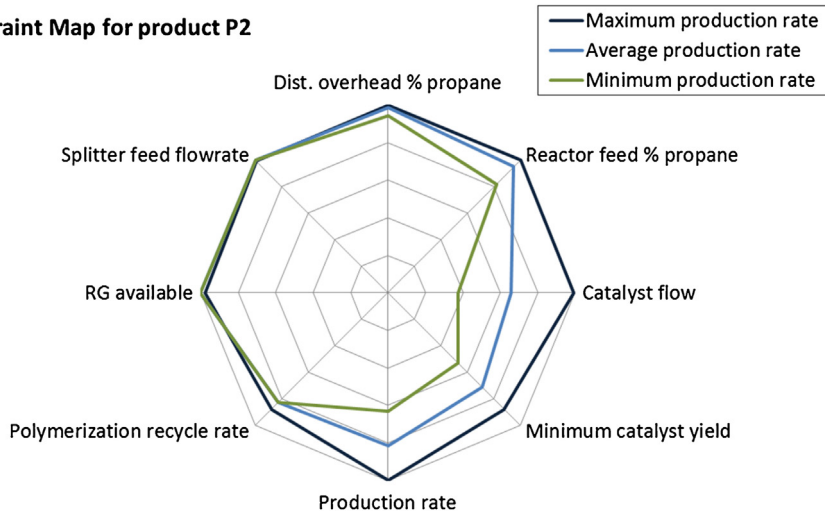
The model size and CPU time, similar for every case, are reported in Table 1. For each product and production rate (a)–(c), Table 3 includes the percentage of propylene coming from the RG feed, together with the composition of propylene at the reactor feed and a normalized profit rate. At lower production rates more propylene from RG is used to feed the distillation unit while assuring the required composition at the reactor feed (maximum 21% propane weight). The percentage of propylene from RG is also shown in Fig. 8.

In order to give some insight on the model behavior, it is instructive to look at the constraints to see which limits are hit under each operating scenario. Figs. 9 and 10 show the constraint maps of product P₁ and P₂, respectively, for each production rate. The values on Figs. 9 and 10 are scaled such that any value along the outer edge of the “spider-web” means the system is at the constraint maximum (or at the minimum, for the specific case of the catalyst yield).

We briefly discuss the constraint map shown in Fig. 9 for product P₁. Low MFI products require higher reactor feed purity and run at lower production rate than high MFI products because they feature lower catalyst yields (determined from the kinetic parameters K_p and KD_p). Increasing the catalyst yield requires increasing the monomer concentration or the residence time, both of which indirectly reduce the production rate. In contrast, increasing the catalyst flow will increase the production rate and decrease the residence time. For fixed production rates, as shown in Fig. 9, the best operating conditions calculated by the model will select as much (cheaper) RGP feed as possible to reduce the total cost, driving the catalyst yield to its minimum. It can be observed in Fig. 9 that the reactor feed propane composition is always relatively far from its upper limit (i.e., higher monomer concentration), the catalyst flow never reaches its maximum rate, and the catalyst yield (lb. PP/lb. catalyst) is close to its minimum for each production rate

Table 3Comparison of single product model results for products P₁ and P₂ at different rates.

Production rate	Product P ₁ (low MFI)			Product P ₂ (high MFI)		
	Minimum	Average	Maximum	Minimum	Average	Maximum
Propylene from RG feed (%)	86.1	76.5	65.0	86.1	66.8	53.3
Reactor feed propylene composition (%)	82.8	82.9	85.1	82.8	80.1	79.0
Normalized profit rate	135.4	143.9	149.7	100.0 ^a	114.3	127.4

^a Reference value.**Constraint Map for product P₁****Fig. 9.** Constraint map for product P₁ at various production rates.**Constraint Map for product P₂****Fig. 10.** Constraint map for product P₂ at various production rates.

analyzed. The constraint maps also show how under different operating conditions the solution moves towards different constraints. For example, when product P₁ is run at minimum rate the RGP flow and splitter feed are both on their maximum capacities. In contrast, when P₁ is run at maximum rate the catalyst yield and monomer recycle to distillation both reach their operation limits.

The normalized profit rates reported in Table 3 were determined by using the minimum profit rate of product P₂ as the reference value. As observed in Fig. 11, the profit rate of P₁ at minimum production rate is higher than the corresponding rate of P₂ at maximum rate. This is consistent because P₁ has a higher price, and

therefore a higher contribution margin per pound than P₂. If products P₁ and P₂ are both scheduled in a fixed time interval, the model needs to balance the production rates and operating conditions to obtain the best overall profit. For example, if the schedule requirements are 50% of P₁ and 50% of P₂, the best solution could be to maximize the production rate of P₂ and select the lowest possible production rate of P₁ (with its highest profit rate) for the time remaining. In this way, the whole time interval is used and the overall profit is maximized. Case studies showing the application of the multiple product model are presented next.

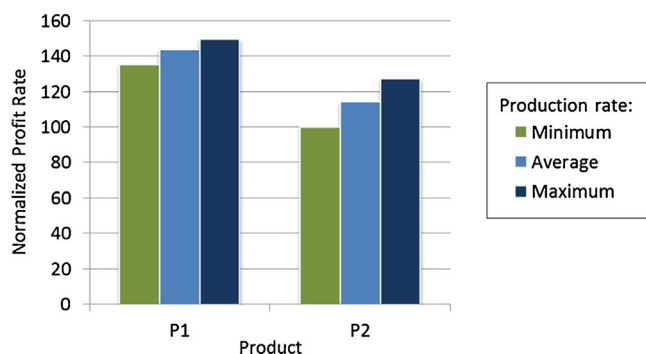


Fig. 11. Normalized profit rates for products P₁ and P₂ considering different production rates.

5.2. Medium term test case: trade-off between feedstock costs and production rates

In this section, the multiple-product feedstock optimization model is applied to find the best operating conditions for a schedule of products, considering a time frame of approximately one month. A test case with 20 products belonging to 6 product families is presented. The schedule demands include a total of 200 railcars (190,000 lbs each), which are shown for each product and product family in Fig. 12. Feedstock prices are the same as in Section 5.1.

5.2.1. Comparison of alternative time horizons

In order to analyze the trade-off between feedstock costs and production rates, alternative time horizons are considered ($H = 27, 30, 34$, and 40 days). To this end, the multiple-product model 2 is solved using different time limits in Eq. (42.6). As discussed in Section 4.2, the solution method aggregates/disaggregates the products by family, and the model simultaneously determines the best operating conditions for each family. The model statistics and CPU time required to aggregate/initialize and solve model 2 are reported in Table 2.

Four main results are analyzed: (i) the production schedule, (ii) the production rate variations (plant load from 0 to 100%), (iii) the percentage of propylene coming from refinery grade (RG) and chemical grade (CG) feedstocks, and (iv) the normalized profit.

Fig. 13 shows the Gantt charts obtained for each time horizon. The model selects different production times for each product, as long as the required volumes are produced and the available time limit is not exceeded. If enough time is available, some products

are run at lower rates in order to reduce the total cost. While the schedule finishes just in time for the first three time horizons, when $H = 40$ days the schedule finishes earlier. In this case, the production plan is completed in 38.62 days with the plant always running at minimum rate. The detailed production rate profiles are shown in Fig. 14. The production rates are reported as a percentage of the maximum rate (which is the same for all products). The model is capable to increase (or decrease) the rate of production, while decreasing (or increasing) the production time, in order to provide a better objective function value. The optimal solution simultaneously balances the production rates and the use of feedstocks for all products, so that the maximum economic return is obtained.

Table 4 includes the percentage of propylene from RG, the average plant production rate, and a normalized profit for each value of H . It can be observed that the profit increases as more time is available to complete the schedule, since at lower rates the distillation unit can extract more propylene from the RG feed, decreasing the feedstock cost. The propylene from RG varies from 60.2% at high production rates to 86.1% at the lowest rate. However, once every product is run at minimum rate, even if more time is available (i.e. with values of H higher than 38.62 days) the profit cannot be improved.

While for large time horizons and low production rates the model predicts the most profitable operating conditions, in these conditions the plant capacity is underutilized. The profit can also be improved by adding some extra production, as shown in the next section.

5.2.2. Extra production or “flexible plans”

An alternative scenario is the possibility of having some extra production at the end of the schedule. In this case, an average “slack” product is considered and model 3 is used with the additional time slot k^* to account for extra production. The amount to be produced is a variable to be determined by the model.

For the extra production scenario we set $H = 30$ days as the reference time horizon. The model statistics and CPU time for model 3 are also reported in Table 2. Besides, the last column of Table 4 includes the plant operating conditions and normalized profit. As shown in Table 4, while the production rate increases and the monomer feed from RG decreases, an additional 6.7% of total profit is obtained. Figs. 15 and 16 compare the schedule and production rates profiles for $H = 30$, with and without considering the extra production. When the “slack” product is considered the plant operates at maximum rate to accommodate additional time at the end of the schedule. This time (3.54 days) is utilized to produce 26.7 rail-

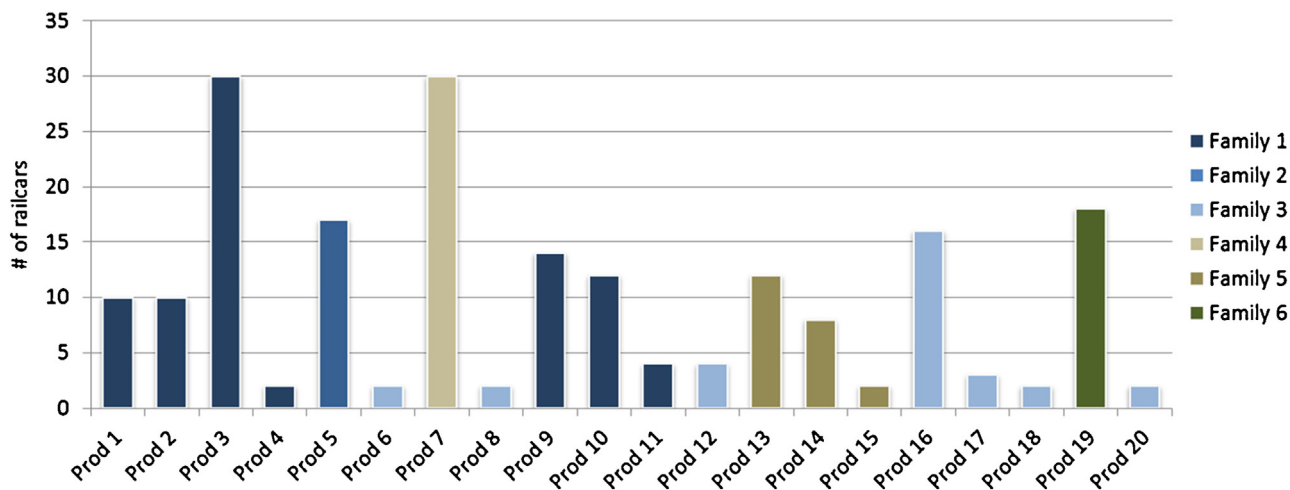
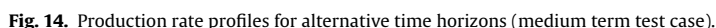


Fig. 12. Production demands for each product/family for the medium term test case.



	Model 2				Model 3
	27 days	30 days	34 days	40 days	30 days w/slack
Propylene from RG feed (%)	60.2	67.0	75.9	86.1	58.5
Plant average production rate (%)	98.0	88.2	77.8	68.5	99.9
Normalized profit	95.7	100.0 ^a	105.6	112.0	106.7

cars of the “slack” product p^* . Even when production costs increase because more CG is used, the overall economic return is compensated by the potential selling price of the extra production. Thus, the results consistently show the desirability of operating the plant at its maximum rate to increase the overall profit.

In this section a long term case study including 22 products belonging to 10 product families is analyzed. The schedule represents a projected annual product slate for a real polypropylene facility, with a total time horizon of 345 days (assuming a planned outage and unplanned downtime). In this test case, instead of a detailed schedule, only the most representative products are selected and the total annualized number of cars of each product is used. We assume that the product prices and feedstock costs

	Cost A	Cost B
PGP marker	72.5	64.0
CGP-PGP spread	1.5	1.5
RGP-PGP spread	9.0	19.6

The multiple-product model is solved considering two scenarios with different feedstock costs (see [Table 5](#)) in order to analyze the sensitivity of having different market conditions. These scenarios represent two months of actual operation. For each scenario, the possibility of having extra production at the end of the schedule is also considered.

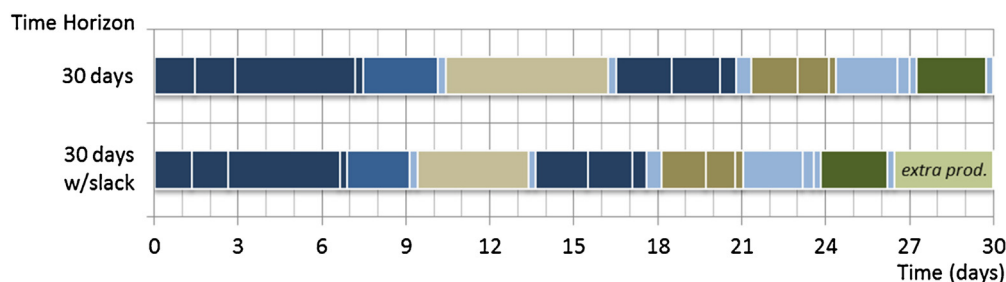


Fig. 15. Optimal schedules with/without additional production (medium term test case).

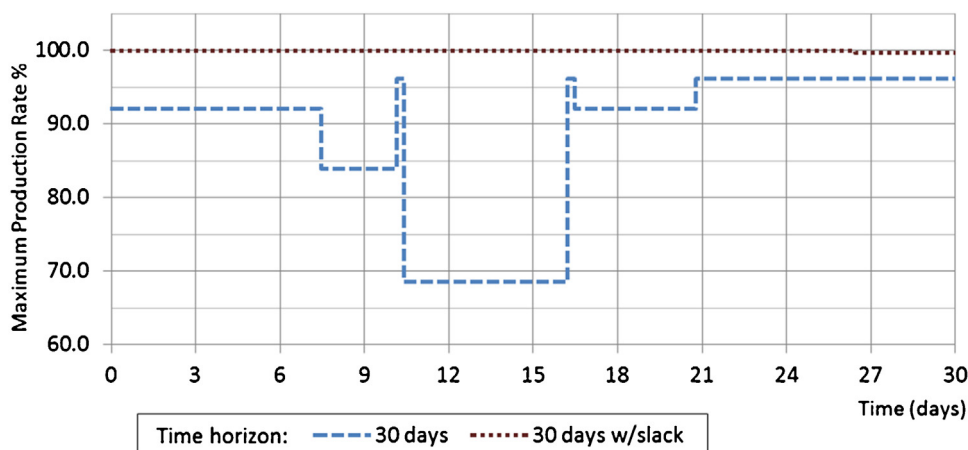


Fig. 16. Comparison of production rate profiles for extra production (medium term test case).

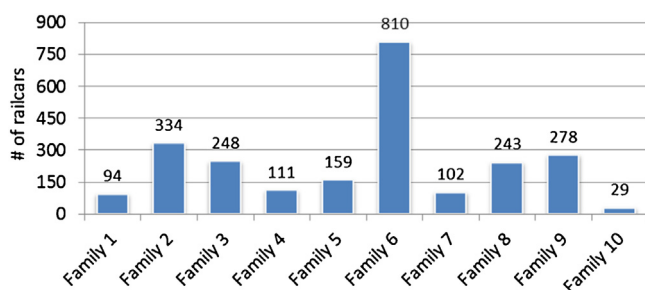


Fig. 17. Long term case study demands for each product family.

The multiproduct feedstock optimization model includes 10 time slots (one for each product family) for model 2, and 11 time slots for model 3, since in the latter a “slack” product is considered. Model statistics and CPU times are given in Table 2. Model results for each product family on each scenario are presented in Figs. 18–21. For comparison, an historical average solution based on actual plant operation data is also included.

Fig. 18 shows the production rates as a percentage of the plant capacity. It can be noted that Families 1 to 4 and Family 10 feature lower maximum production rates when compared with the plant maximum. For each family, the production rates obtained with model 2 are either higher or lower than the corresponding average historical rates. In contrast, when additional production is allowed, the production rates of all families are (usually) at their maximum capacities. In general, the multiple-product schedules fill the entire time horizon, a condition that is achieved by running slower (model 2) or running faster and producing extra product (model 3). Some differences can also be observed between the solutions by considering the alternative feedstock costs. In particular, the production rates of model 3 (accounting for extra production)

are higher when optimized using feedstock costs A, compared with the usage of feedstock costs B. In this case, 111.5 additional railcars of “slack” product (case A) versus 95.9 railcars (case B) are produced.

Fig. 19 includes the percentage of the RG capacity selected for each family and model solution (refinery grade is received by pipeline with a maximum feedrate). It can be observed that the solutions of model 2 always use the maximum feedrates of RG, while lower rates are used when extra production is considered (model 3). Fig. 20 shows the fraction of propylene obtained from the RG feed in each case. As expected, at lower rates (model 2) more propylene is sourced from the refinery grade feed, and at higher rates (model 3 with “slack” production) less monomer from RG is used.

Table 6 summarizes the operating conditions obtained by the multiple product models 2 and 3. Results in Table 6 are averaged by volume, and the historical solution is also included. While the solutions of model 2 are not the same for feedstock costs A and B, they are similar and present almost the same average values.

A comparison of normalized profit rates is included to illustrate the potential economic impact of the proposed method. To this end, the operating conditions of the historical solution with feedstock costs A are used to determine an average profit rate for the schedule. This profit rate is normalized as the reference value in Table 7 (N\$

Table 6
Plant operating conditions for alternative solutions of the multiple-product long term case study.

	Historical average	Model 2	Model 3 (extra prod.)	
		Cost A & B	Cost A	Cost B
Average production rate (%)	92.64	92.64	96.87	96.34
RG feed capacity used (%)	95.53	100.00	98.59	99.19
Propylene from RG feed (%)	61.20	64.06	60.37	61.12

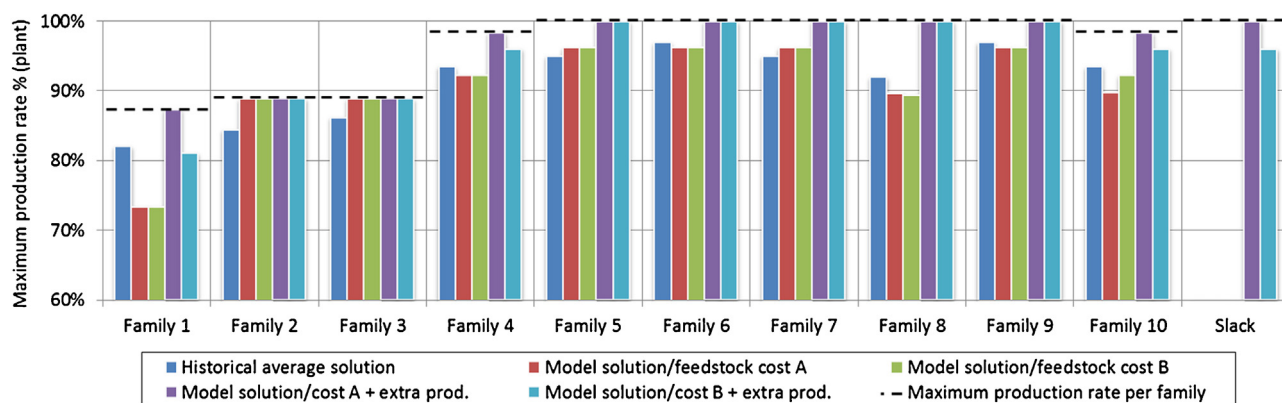


Fig. 18. Production rates for each product family and solution of the long term case study.

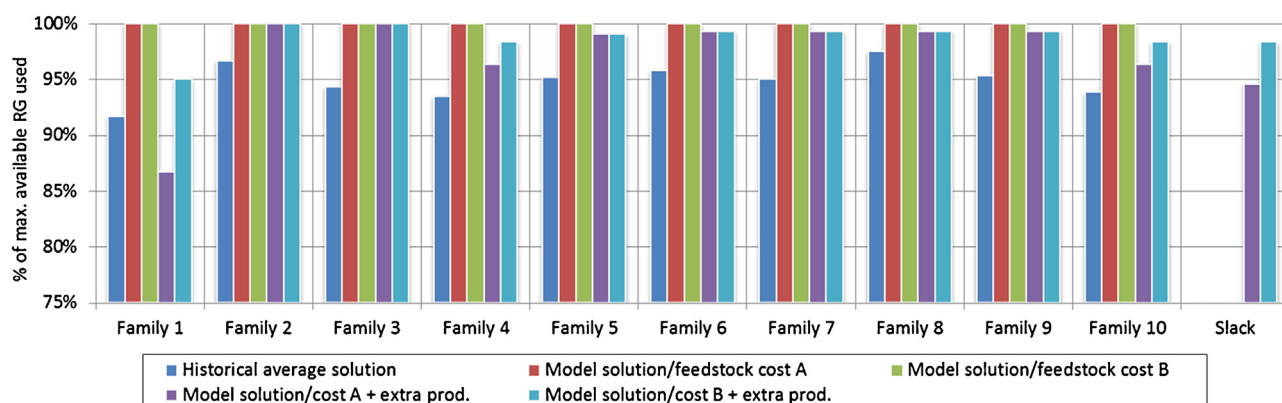


Fig. 19. Percentage of maximum RG feedrates for the long term case study.

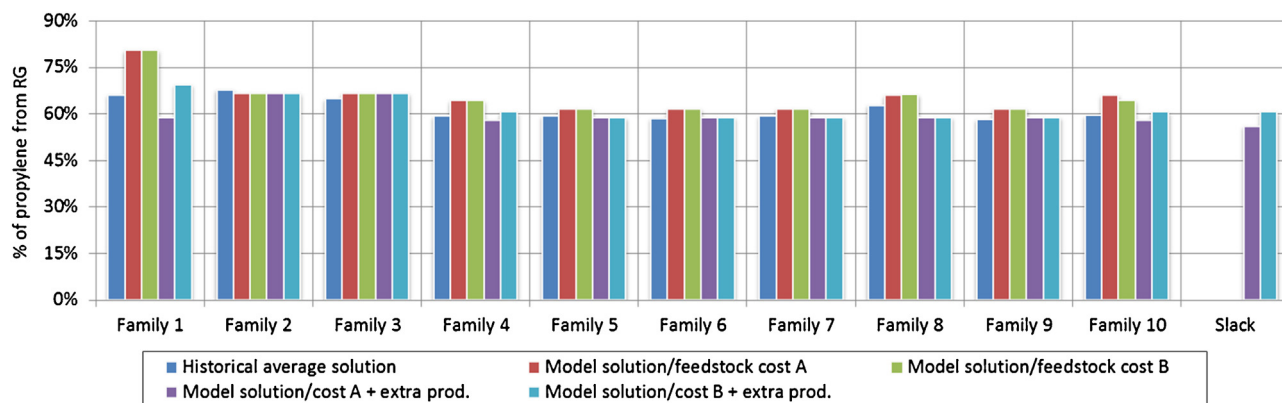


Fig. 20. Propylene fraction from RG feed for each product family and solution of the long term test case.

Table 7
Comparison of normalized profit rates (N\$/h) for long term case study.

	Cost A	Cost B
Historical average solution	100.00 ^a	161.21
Model 2 solution	101.63	165.96
Model 3 solution w/slack product	104.50	167.77

^a Reference value.

stands for the monetary unit). Thus, a rate of 100 N\$/h means that the actual profit is 828,000 N\$, because the time horizon includes 8280 h (345 days).

Table 7 shows that a larger overall profit is obtained when the feedstock mix is optimized. For feedstock costs A, the solution with the multiple-product model 2 exhibits a 1.63% increase compared

with the historical solution. In turn, when extra production is considered (model 3), an increase of 4.5% is found. If the same analysis is made for feedstock costs B, the increases are 2.95% and 4.07% for models 2 and 3, respectively (using 161.21 as reference value). Besides, by comparing the solutions of models 2 and 3, the results consistently show that additional profit can be obtained by running the plant at maximum rate to gain time for extra production (similar to the extra production scenario presented in Section 5.2.2). The detailed profit rates for each product family are shown in Fig. 21.

To give an idea of the actual economics, if we use the rate 1 N\$ = 50 dollars, the solutions of model 2 represent an annualized additional profit of \$674,820 and \$1,966,500 for feedstock costs A and B, respectively, when compared with the historical average solution where the feedstock mix is not optimized. In turn, the

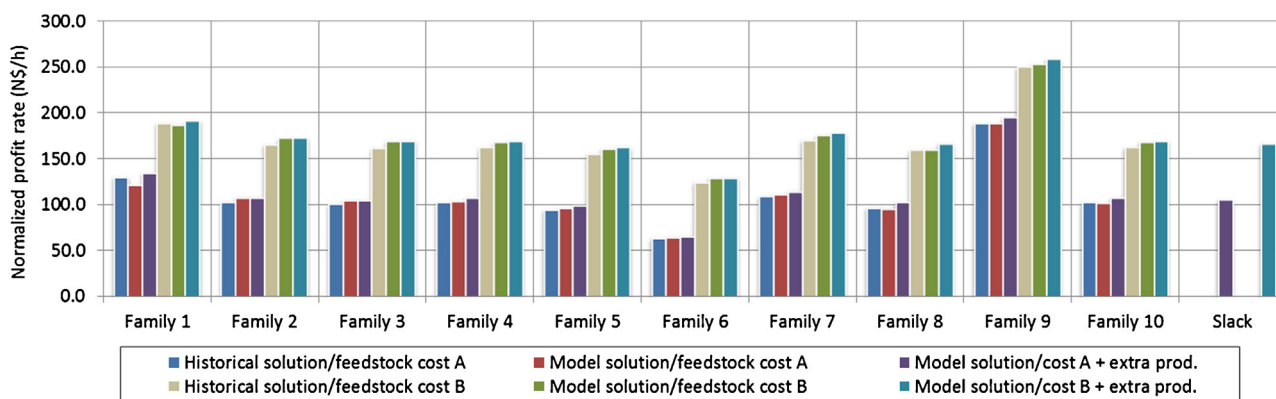


Fig. 21. Normalized profit rates for long term case study.

additional profit attainable by adding extra production (model 3) is \$1,863,000 and \$2,715,840, respectively.

Finally, it is important to mention that there can be some revenue loss associated with operating at the same conditions under different feedstock costs. To give an example, if the market operates with feedstock costs A but we use the solution of model 3 optimized with feedstocks cost B, the profit rate decreases to 104.22 N\$/h. Using the rate 1 N\$ = 50 dollars, this represents an annual loss of \$115,920. Conversely, if the market conditions are given by cost B but the solution of model 3 is obtained with cost A, the profit rate decreases to 167.6 N\$/h (with an annual loss of \$70,380). These results suggest that there is a clear advantage in using the model to obtain the best operating conditions while taking into account the feedstock costs.

6. Conclusions

Both single and multiple-product nonlinear programming models for optimal production planning and feedstock mix selection at a polypropylene production facility have been developed. The process under study includes a distillation unit and a polymerization loop reactor, and the feedstocks are refinery and chemical grade propylene. The single product model is able to find the best economic return and steady state operating conditions for a given product, by using a simplified representation of the process units. On the one hand, the distillation column is represented using an aggregated group-method to reduce the model's size and complexity, given the large number of trays that an exact approach would demand. While modelling cascades of trays instead of individual trays, the group-method provides accurate estimations of the splitter's behavior. On the other hand, a simplified nonlinear Ziegler-Natta polymerization model describing the reactor has been used, which is based on parameters calculated from plant data. Built upon the single-product model, and considering the additional variable of time, the proposed multiple-product formulation is able to optimize the economic return of a schedule of polymer products within a given time horizon. Besides, it considers the possibility of adding "extra" production at the end of the schedule. For both models, initialization strategies were proposed in order to increase the robustness of the nonlinear optimization. An aggregation/disaggregation approach considering families of products with similar kinetic properties is used.

The proposed formulations have been applied to several case studies, both to analyze the behavior of the model and to illustrate its potential economic impact. Results obtained from the application of the single product model, by considering two products and alternative production rates, explicitly demonstrate that operat-

ing conditions and line economics leading to highest profit are not the same for every product and often lie at one or more system constraints (limits on splitter feed, distillation overhead propylene purity, catalyst yield, etc.)

For the multiple-product formulation, both medium and long term case studies were presented. The optimum solutions usually feature lower production rates for certain products to obtain a better separation on the distillation unit, thus reducing the production cost by using more refinery grade as feed to the column. On the medium term test case different time horizons were tested to establish the tradeoff of decreasing feedstock costs versus increasing the production rate. Besides, a "slack" product was added to assess the benefits of having some extra production when the schedule finishes earlier. This "extra" production is recommended in cases where the line is sold out, but usually not called for in "push" markets where product margins are low. The results consistently show the advantage of running the plant at its maximum capacity whenever possible.

Finally, a long term case study based on an annualized product slate was presented. Comparison of model results with different feedstock costs, versus an average historical solution, show that substantial savings can be gained by adjusting the process conditions and taking a higher fraction of refinery grade feed for some products. The potential additional profit is even higher when "extra" production is considered. Overall, the model shows that using a feedstock mix and operating conditions that are not economically optimal for a given monomer spread can have a large effect on feedstock costs.

The proposed feedstock optimization methodology with a user-friendly spreadsheet-based interface (see Appendix B) has been deployed to support commercial decisions at Braskem. From the commercial point of view, the computational tool is able to assist not only on feedstock purchase decisions for a given slate, but also on multiple types of what-if analysis (line loading plans, product wheel updates, etc.) From the operations point of view, the results can be used to set the operation targets (loop feed purity, distillation overhead purity, production rates, etc.) for each product over time. Several case studies with actual plant data were tested, and the results have shown that annualized potential savings of \$0.4–\$16 MM could be obtained, depending on the monomer spread.

Acknowledgment

The authors would like to acknowledge the financial support received from Braskem America and the Center for Advanced Process Decision Making (CAPD).

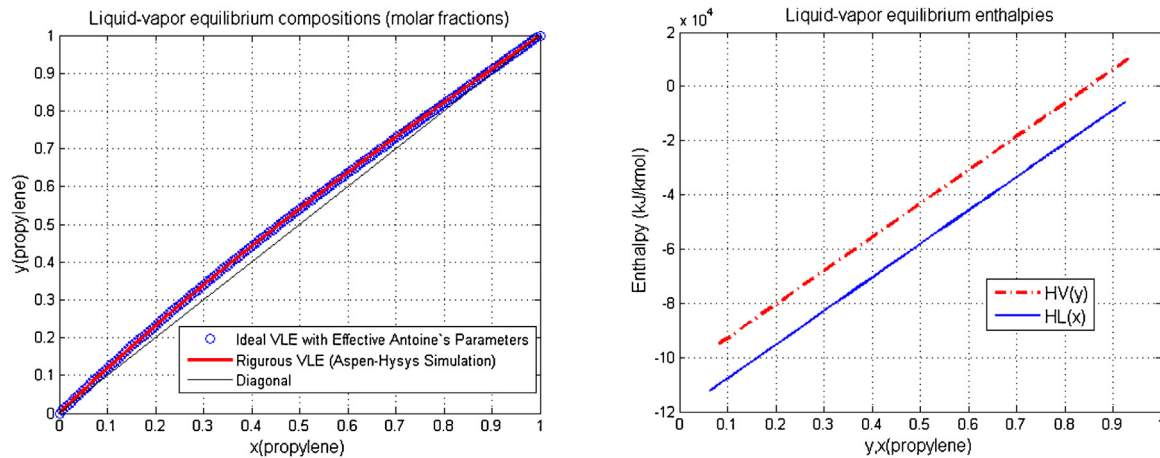


Fig. A1. Liquid-vapor equilibrium data for propylene-propane system.

Appendix A. Calculation of effective parameters for the propane-propylene distillation model

Since the separation of propane-propylene involves very low relative volatilities, the accuracy of vapor-liquid equilibrium correlations is critical (Kister, 2008). In order to improve the performance of the aggregated model used in the present work and the corresponding phase equilibrium calculations, a set of Effective Parameters of the Antoine's Equation have been calculated by correlating the distillation trajectories obtained from rigorous Aspen Hysys simulations of the distillation column under study. As Fig. A1 shows, the system presents an ideal behavior from the liquid-vapor equilibrium point of view, including a linear variation of the enthalpies with the composition of both equilibrium phases.

To validate the effective parameters obtained, they have been used additionally to reproduce the distillation column by using a revision of classical tray by tray methods such as the McCabe-Thiele Method and the Ponchon-Savarit Method (Reyes-Labarta et al., 2014). The results and distillation profiles obtained reproduce satisfactorily the ones obtained from the rigorous Aspen Hysys simulations, confirming the accuracy of the effective Antoine's parameters obtained.

Appendix B. Feedstock optimization computational tool

A user-friendly interface has been developed in MS-Excel to interact with the model (see Fig. B1). By using this interface a practicing engineer can easily define the schedule data and model parameters, and review the model results in different lev-

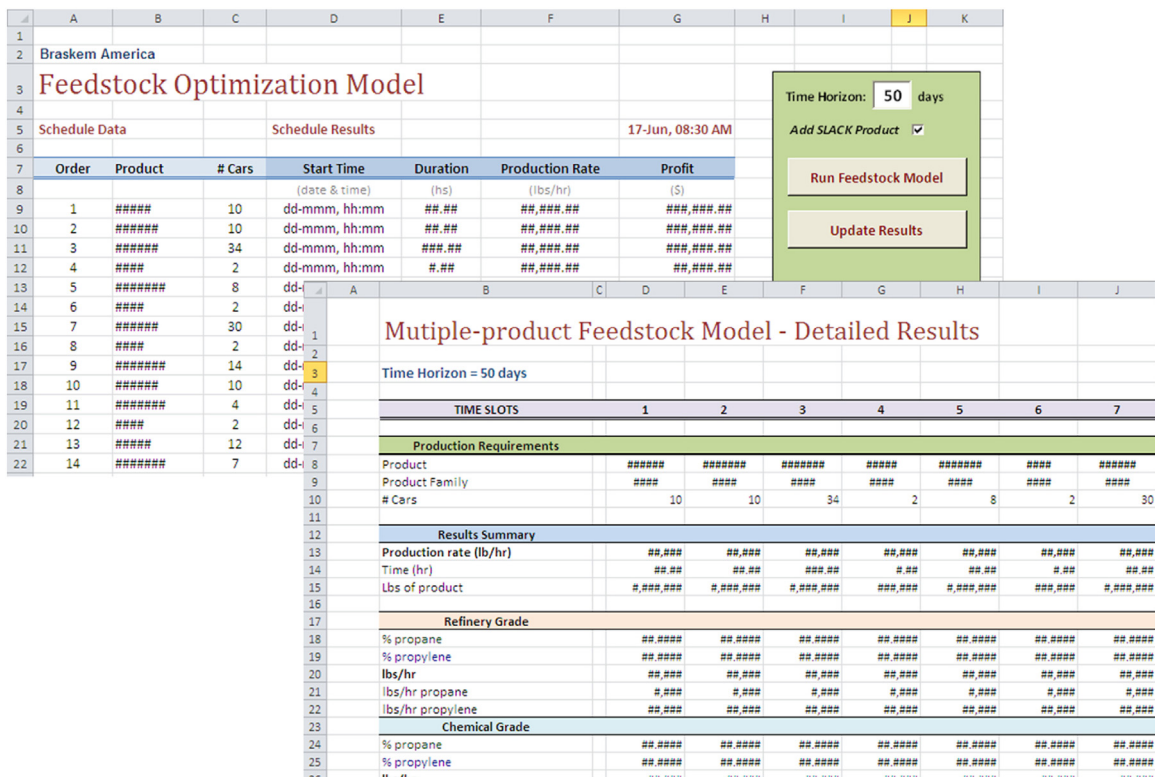


Fig. B1. Feedstock optimization computational tool (user-interface screenshots).

els of detail. This gives the flexibility to test multiple production schedules with different demands and product specifications. The aforementioned tool can be applied to determine production rates for a schedule of multiple production orders within a given time-frame.

References

- Albizzati, E., Cecchin, G., Chadwick, J.C., Collina, G., Giannini, U., Morini, G., et al., 2005. Catalysts for polymerization. In: Pasquini, N. (Ed.), *Polypropylene Handbook*, 2nd ed. Hanser, München, Germany, pp. 15–106.
- Al-haj Ali, M., Betlem, B., Roffel, B., Weickert, G., 2006. Hydrogen response in liquid propylene polymerization: towards a generalized model. *AIChE J.* 52 (5), 1866–1876.
- Almeida, A.S., Wada, K., Secchi, A.R., 2008. Simulation of styrene polymerization reactors: kinetic and thermodynamic modeling. *Braz. J. Chem. Eng.* 25 (2), 337–349.
- Bagajewicz, M.J., Manousiouthakis, V., 1992. Mass/heat-exchange network representation of distillation networks. *AIChE J.* 38 (11), 1769–1800.
- Barttfeld, M., Aguirre, P.A., Grossmann, I.E., 2003. Alternative representations and formulations for the economic optimization of multicomponent distillation columns. *Comput. Chem. Eng.* 27 (3), 363–383.
- Bausa, J., von Watzdorf, R., Marquardt, W., 1998. Shortcut methods for nonideal multicomponent distillation: 1. Simple columns. *AIChE J.* 44 (10), 2181–2198.
- Belotti, P., Kirches, C., Leyffer, S., Linderoth, J., Luedtke, J., Mahajan, A., 2013. Mixed-integer nonlinear optimization. *Acta Numer.* 22, 1–131.
- Biegler, L.T., Zavala, V.M., 2009. Large-scale nonlinear programming using IPOPT: an integrating framework for enterprise-wide dynamic optimization. *Comput. Chem. Eng.* 33, 575–582.
- Biegler, L.T., 2007. An overview of simultaneous strategies for dynamic optimization. *Chem. Eng. Process.* 46, 1043–1053.
- Caballero, J.A., Grossmann, I.E., 1999. Aggregated models for integrated distillation systems. *Ind. Eng. Chem. Res.* 38 (6), 2330–2344.
- Castro, P.M., Harjunkoski, I., Grossmann, I.E., 2009. New continuous-time scheduling formulation for continuous plants under variable electricity cost. *Ind. Eng. Chem. Res.* 48 (14), 6701–6714.
- Fenske, M.R., 1932. Fractionation of straight-run Pennsylvania gasoline. *Ind. Eng. Chem.* 24 (5), 482–485.
- Flores-Tlacuahuac, A., Biegler, L.T., 2008. Integrated control and process design during optimal polymer grade transition operations. *Comput. Chem. Eng.* 32, 2823–2837.
- Floudas, C.A., Lin, X., 2004. Continuous-time versus discrete-time approaches for scheduling of chemical processes: a review. *Comput. Chem. Eng.* 28 (11), 2109–2129.
- Garoff, T., Virkkunen, V., Jääskeläinen, P., Vestberg, T., 2003. A qualitative model for polymerisation of propylene with a MgCl_2 -supported TiCl_4 Ziegler-Natta catalyst. *Eur. Polym. J.* 39, 1679–1685.
- Gilliland, E.R., 1940. Multicomponent rectification: estimation of the number of theoretical plates as a function of the reflux ratio. *Ind. Eng. Chem.* 32 (9), 1220–1223.
- Grossmann, I.E., 2005. Enterprise-wide optimization: a new frontier in process systems engineering. *AIChE J.* 51 (7), 1846–1857.
- Grossmann, I.E., 2012. Advances in mathematical programming models for enterprise-wide optimization. *Comput. Chem. Eng.* 47, 2–18.
- Harjunkoski, I., Maravelias, C.T., Bongers, P., Castro, P.M., Engell, S., Grossmann, I.E., Hooker, J., Méndez, C., Sand, G., Wassick, J., 2014. Scope for industrial applications of production scheduling models and solution methods. *Comput. Chem. Eng.* 62, 161–193.
- Jackson, J.R., Hofmann, J., Wassick, J., Grossmann, I.E., 2003. A nonlinear multiperiod process optimization model for production planning in multi-plant facilities. In: Grossmann, I.E., McDonald, C.M. (Eds.), *Proceedings of FOCAPO 2003*, 281–284.
- Kadipasaoglu, S., Captain, J., James, M., 2008. Polymer supply chain management. *Int. J. Logist. Syst. Manage.* 4 (2), 233–253.
- Kamath, R.S., Grossmann, I.E., Biegler, L.T., 2010. Aggregate models based on improved group methods for simulation and optimization of distillation systems. *Comput. Chem. Eng.* 34 (8), 1312–1319.
- Kiparissides, C., 1996. Polymerization reactor modeling: a review of recent development and future directions. *Chem. Eng. Sci.* 51 (10), 1637–1659.
- Kiparissides, C., 2006. Challenges in particulate polymerization reactor modeling and optimization: a population balance perspective. *J. Process Control* 16, 205–224.
- Kissin, Y.V., 2003. Multicenter nature of titanium-based Ziegler-Natta catalysts: comparison of ethylene and propylene polymerization reactions. *J. Polym. Sci. Part A: Polym. Chem.* 41 (12), 1745–1758.
- Kister, H.Z., 2008. Effects of design on tray efficiency in commercial towers. *Chem. Eng. Prog.* 104 (6), 39–47.
- Kolodziej, S.P., Grossmann, I.E., Furman, K.C., Sawaya, N.W., 2013. A discretization-based approach for the optimization of the multiperiod blend scheduling problem. *Comput. Chem. Eng.* 53, 122–142.
- Kondili, E., Pantelides, C.C., Sargent, R.W.H., 1993. A general algorithm for short-term scheduling of batch operations-I. MILP formulation. *Comput. Chem. Eng.* 17 (2), 211–227.
- Kremser, A., 1930. Theoretical analysis of absorption process. *Nat. Petrol. News* 22, 43–49.
- Lin, W., Biegler, L.T., Jacobson, A.M., 2010. Modeling and optimization of a seeded suspension polymerization process. *Chem. Eng. Sci.* 65 (15), 4350–4362.
- Mahadevan, R., Doyle III, F.J., Allcock, A.C., 2002. Control-relevant scheduling of polymer grade transitions. *AIChE J.* 48 (8), 1754–1764.
- Matos, V., Mattos Neto, A.G., Pinto, J.C., 2001. Method for quantitative evaluation of kinetic constants in olefin polymerizations: I. Kinetic study of a conventional Ziegler-Natta catalyst used for propylene polymerizations. *J. Appl. Polym. Sci.* 79, 2076–2108.
- Matos, V., Mattos Neto, A.G., Nele, M., Pinto, J.C., 2002. Method for quantitative evaluation of kinetic constants in olefin polymerizations: II. Kinetic study of a high-activity Ziegler-Natta catalyst used for bulk propylene polymerizations. *J. Appl. Polym. Sci.* 86, 3226–3245.
- McKenna, T.F., Soares, J.B.P., 2001. Single particle modelling for olefin polymerization on supported catalysts: a review and proposals for future developments. *Chem. Eng. Sci.* 56 (13), 3931–3949.
- Méndez, C.A., Cerdá, J., Grossmann, I.E., Harjunkoski, I., Fahl, M., 2006a. State-of-the-art review of optimization methods for short-term scheduling of batch processes. *Comput. Chem. Eng.* 30 (6–7), 913–946.
- Méndez, C.A., Grossmann, I.E., Harjunkoski, I., Kaboré, P., 2006b. A simultaneous optimization approach for off-line blending and scheduling of oil-refinery operations. *Comput. Chem. Eng.* 30 (4), 614–634.
- Mouret, S., Grossmann, I.E., Pestiaux, P., 2009. A novel priority-slot based continuous-time formulation for crude-oil scheduling problems. *Ind. Eng. Chem. Res.* 48 (18), 8515–8528.
- Nocedal, J., Wright, S.J., 2006. *Numerical Optimization*, Second ed. Springer, New York.
- Pinto, J.M., Grossmann, I.E., 1994. Optimal cyclic scheduling of multistage continuous multiproduct plants. *Comput. Chem. Eng.* 18 (9), 797–816.
- Reginato, A.S., Zacca, J.J., Secchi, A.R., 2003. Modeling and simulation of propylene polymerization in nonideal loop reactors. *AIChE J.* 49 (10), 2642–2654.
- Reyes-Labarta, J.A., Serrano, M.D., Marcilla, A., 2014. Analysis of the connecting zone between consecutive sections in distillation columns covering multiple feeds, products and heat transfer stages. *Latin Am. Appl. Res.* 44 (4), 307–312.
- Soares, J.B.P., 2001. Mathematical modelling of the microstructure of polyolefins made by coordination polymerization: a review. *Chem. Eng. Sci.* 56 (13), 4131–4153.
- Sundaramoorthy, A., Maravelias, C.T., 2011. Computational study of network-based mixed-integer programming approaches for chemical production scheduling. *Ind. Eng. Chem. Res.* 50 (9), 5023–5040.
- Terrazas-Moreno, S., Flores-Tlacuahuac, A., Grossmann, I.E., 2007. Simultaneous cyclic scheduling and optimal control of polymerization reactors. *AIChE J.* 53 (9), 2301–2315.
- Touloupides, V., Kanellopoulos, V., Pladis, P., Kiparissides, C., Mignon, D., Van-Grambezen, P., 2010. Modeling and simulation of an industrial slurry-phase catalytic olefin polymerization reactor series. *Chem. Eng. Sci.* 65, 3208–3222.
- Viswanathan, J., Grossmann, I.E., 1993. An alternate MINLP model for finding the number of trays required for a specified separation objective. *Comput. Chem. Eng.* 17 (9), 949–955.
- Wu, D., Ierapetritou, M., 2004. Cyclic short-term scheduling of multiproduct batch plants using continuous-time representation. *Comput. Chem. Eng.* 28 (11), 2271–2286.
- Yeomans, H., Grossmann, I.E., 2000. Optimal design of complex distillation columns using rigorous tray-by-tray disjunctive programming models. *Ind. Eng. Chem. Res.* 39 (11), 4326–4335.
- You, F., Castro, P.M., Grossmann, I.E., 2009. Dinkelbach's algorithm as an efficient method to solve a class of MINLP models for large-scale cyclic scheduling problems. *Comput. Chem. Eng.* 33 (11), 1879–1889.
- Zacca, J.J., Debling, J.A., Ray, W.H., 1996. Reactor residence time distribution effects on the multistage polymerization of olefins—I. Basic principles and illustrative examples, polypropylene. *Chem. Eng. Sci.* 51 (21), 4859–4886.
- Zavala, V.M., Biegler, L.T., 2009. Optimization-based strategies for the operation of low-density polyethylene tubular reactors: nonlinear model predictive control. *Comput. Chem. Eng.* 33, 1735–1746.